Cyclical Tests of Selected

Space Shuttle TPS Metallic Materials

in a Plasma Arc Tunnel

Volume I - Description of Tests and Program Summary

W.A. Rinehart
D.W. Land
J.H. Painter
R.A. Williamson

MCDONNELL DOUGLAS RESEARCH LABORATORIES

MCDONNELL DOUGLAS

CORPORATION

Final Report

Cyclical Tests of Selected Space Shuttle TPS Metallic Materials in a Plasma Arc Tunnel

Volume I - Description of Tests and Program Summary

by
W.A. Rinehart, D.W. Land, J.H. Painter, and R.A. Williamson

Flight Sciences Department
McDonnell Douglas Research Laboratories
McDonnell Douglas Corporation
St. Louis, Missouri 63166

MCDONNELL DOUGLAS

Foreword

The work described herein was performed by the McDonnell Douglas Research
Laboratories under NASA Contract NAS2-6601. The NASA Technical Monitor
was N.S. Vojvodich, Research Scientist, Thermal Protection Branch, NASA Ames
Research Center. This report is divided into two volumes. The first volume
contains the main text describing the work performed and a discussion of the
results. The second volume, the appendices (NASA CR 114520), contains the
calibration data, the model temperature histories, and the model physical
measurements.

Contents

This document consists
of a title page, pages iii and v
and pages 1 through 49.

1 Abstract

The work described in this report concerned the cyclical thermal evaluation of selected space shuttle thermal protection system (TPS) metallic materials in a hypervelocity oxidizing atmosphere that approximated an actual entry environment. A total of 325 sample test hours were conducted in the McDonnell Douglas Research Laboratories (MDRL) Plasma Arc Tunnel (PAT) facility on 21 super-alloy metallic samples at temperatures from 1800 to 2200°F (1256 to 1478 K) without any failures. The 4 x 4 in. (10.2 x 10.2 cm) samples were fabricated from five nickel base alloys and one cobalt base alloy. Eighteen of the samples were cycled 100 times each and the other three samples 50 times each in a test stream emanating from an 8 in. (20.3 cm) diam exit, Mach 4.6, conical nozzle. The test cycle consisted of a 10 min heat pulse to a controlled temperature followed by a 10 min cooldown period.

Measurements of sample temperature were obtained with both physical and optical techniques. Each sample was instrumented on the backface with five tack-welded thermocouples after errors of several hundred degrees were found in early tests utilizing spring-loaded thermocouples. In addition, an optical pyrometer and a scanning infrared imaging system were used to measure the sample front face temperature distribution. Measurements of total normal emittance using an emissometer were made on strips of the various materials at typical steady-state test conditions. Measurements of weight and thickness changes were made at periodic intervals for each sample. The TD-NiCrAl and TD-NiAlY materials showed the least change in weight, thickness, and physical appearance even though they were subjected to the highest temperature environment.

2 Introduction

A broad cross-section of materials including metallic radiators, surface insulators, ablators, and carbon-carbon composites have been suggested for the entry thermal protection system (TPS) of the proposed space shuttle vehicle. Several candidate metallic materials are being considered for use on the space shuttle in regions where the reentry heating is moderate [maximum temperatures less than $2200^\circ F$ (1478 K)]. Among these materials are the nickel base alloys which have been dispersed with thoria to improve their high temperature properties. The purpose of this work was to evaluate large samples [4 x 4 in. (10.2 x 10.2 cm)] of the more promising metallic radiators by cyclical testing in a hypervelocity oxidizing atmosphere that approximated an actual entry environment. It was desired to obtain the maximum model size and still maintain a uniform test stream. Multiple holders designed for ease in model change were used to maximize efficiency and minimize test cost. No previous work of this nature has been reported involving either samples this large or total test times as long as 1000 min.

All tests were performed in the supersonic air test stream of the McDonnell Douglas Research Laboratories (MDRL) Plasma Arc Tunnel (PAT) facility located in St. Louis, Missouri. The test period extended from December 1971 to April 1972. Twenty-one metallic samples fabricated from six different alloys were evaluated. Earlier tests on similar materials had been performed in

the PAT facility with the samples at a 60 deg (1.05 rad) angle-of-attack[1]. All tests were conducted during this program with the samples normal to the test stream. This provided a uniform temperature distribution over a larger part of the sample than was experienced during the earlier tests[1].

The nominal test conditions maintained on the samples during each 10 min test cycle included one of three different temperature levels, 1800, 2000, or $2200^\circ F$ (1256, 1367, or 1478 K), at an impact pressure of approximately 6 Torr (800 N/m^2). The samples reached the desired test temperature in less than 30 sec after insertion into the test stream. The sample temperature distribution was continuously measured using several techniques throughout each test cycle. The physical appearance of the sample along with weight and thickness changes were recorded at periodic cycle intervals.

Volume I of this report describes the PAT facility and other apparatus used in the performance of this program. Calibration tests, the sample test technique, and test results are discussed. The predicted thermal performance, analyses of the optical and thermocouple temperature measurements, and emittance measurements are also presented. Additional results such as calibration data, sample physical changes, and measured temperature distributions are presented in Volume II.

3 Apparatus

3.1 Plasma arc tunnel (PAT) facility

The MDRL PAT facility (Fig. 1) consists of an arc heater, model actuator, 6 ft (1.8 m) diam, 27 ft (8.2 m) long, water-cooled vacuum tank, six-stage steam ejector system, power, water, and air supplies, plus associated instrumentation. Figure 2 shows the operating range used on this program along with the PAT facility test stream capabilities for the splash-type test configuration.

The arc heater used in the PAT facility is a Huls-type, dc powered arc heater with tandem, water-cooled, cylindrical hollow electrodes. Two

600 kW power supplies are used for operating the arc heater. Each supply is a three-phase, full-wave rectifier and has a saturable reactor current control. Table 1 shows the range of arc heater operating parameters. In this type of arc heater, the largest percentage of electrode erosion occurs during arc heater start-up and stabilization; therefore, the ability to operate the arc heater continuously for long periods at constant conditions results in sizeable reductions in total electrode erosion. For this program the total contamination caused by electrode erosion was only 0.02% by weight. The electrode material used for this program was a 20% Cu - 80% Ag alloy.

Several nozzles are available for use with the PAT facility. The exit diameters range from 1.25 to 8.0 in. (3.17 - 20.3 cm). They are all conical convergent-divergent nozzles and provide super-sonic flow up to Mach 5.9. The nozzle used for this program had an 8.0 in. (20.3 cm) diam exit with a 1.00 in. (2.54 cm) diam throat, and pro-vided Mach 4.6 flow at the nozzle exit.

The water-cooled model actuator system in the PAT facility accommodates up to three test models per facility run. The model actuator arms are spaced 90 deg (1.57 rad) apart and can be indexed into the test stream either clockwise or counter-clockwise. The axial position of the entire system can be varied 12 in. (30.5 cm) during a run. Each model arm position is indicated electronically on the data recording system to within 0.05 sec of its locked, centerline position.
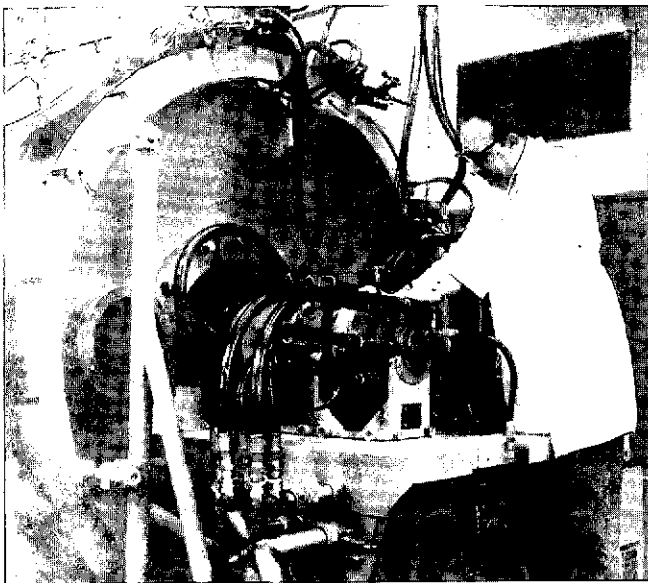

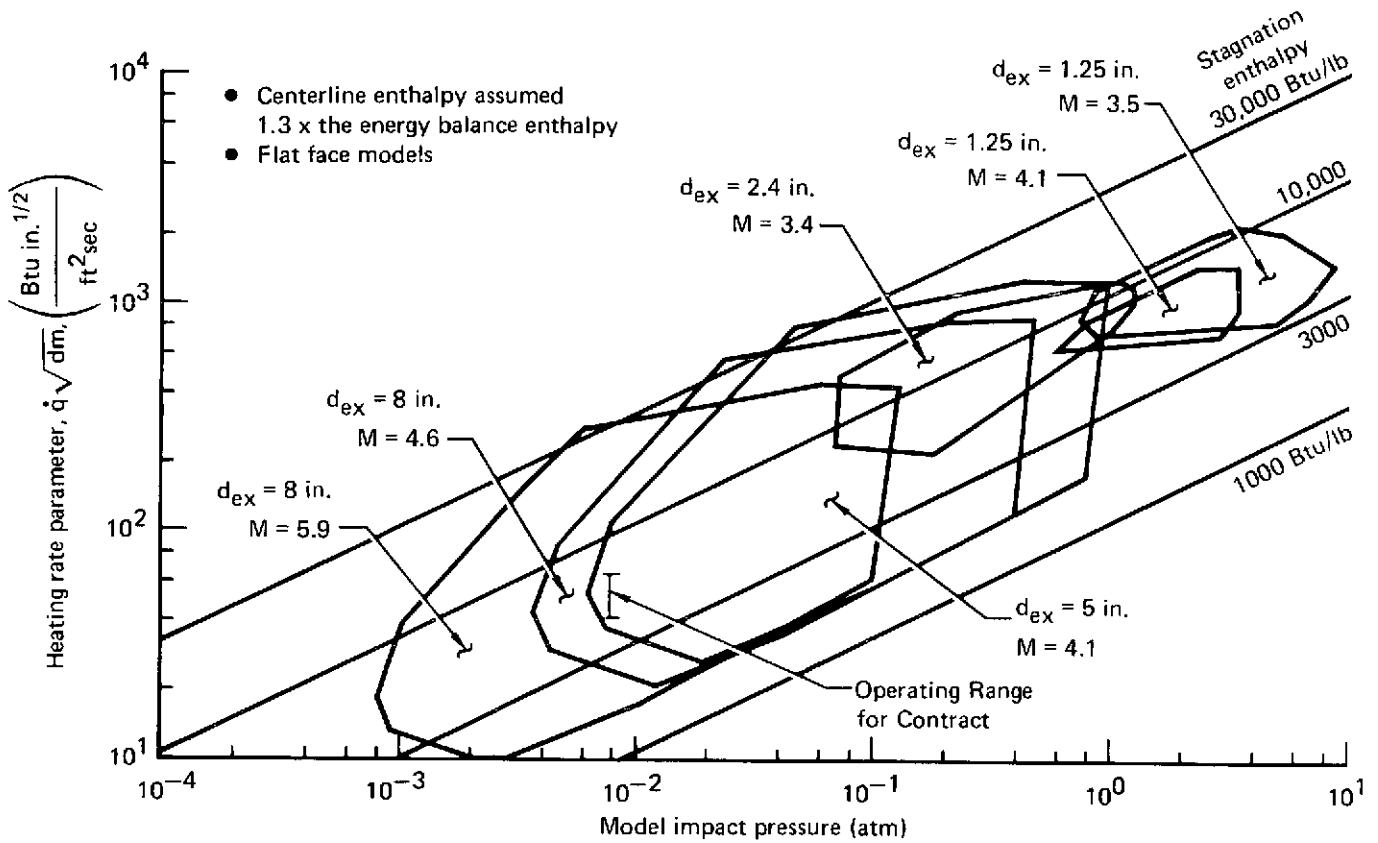**Fig. 1   Plasma arc tunnel (PAT) facility**

GP73-0587-1

Fig. 2 graph labels:

- Centerline enthalpy assumed 1.3 x the energy balance enthalpy
- Flat face models

$d_{ex} = 1.25$ in. M = 3.5

$d_{ex} = 1.25$ in. M = 4.1

$d_{ex} = 2.4$ in. M = 3.4

Stagnation enthalpy 30,000 Btu/lb

10,000

3000

1000 Btu/lb

$d_{ex} = 8$ in. M = 4.6

$d_{ex} = 8$ in. M = 5.9

$d_{ex} = 5$ in. M = 4.1

Operating Range for Contract

Y-axis: Heating rate parameter, $\dot{q}\sqrt{dm}$, $\left(\dfrac{Btu\ in.^{1/2}}{ft^2 sec}\right)$

X-axis: Model impact pressure (atm)

Fig. 2 PAT facility splash testing capability

GP73-0587-2

Table 1 PAT facility arc heater operating range

Parameter	Range of operation	Operating parameters at		
		Maximum bulk enthalpy	Maximum chamber pressure	Maximum power input
Bulk enthalpy (Btu/lb)	2000 - 29,000	29,000	2800	3400
Chamber pressure (atm)	0.09 - 56.5	0.18	56.5	35.8
Power input (MW)	0.065 - 2.33	0.19	1.83	2.33
Air flow rate (lb/sec)	0.0023 - 0.289	0.003	0.238	0.281
Arc current (A)	183 - 2000	620	810	1040
Arc voltage (V)	106 - 2260	305	2240	2240
Efficiency (%)	12 - 71	49	41	45
Nozzle throat diam (in.)	0.250 - 1.000	0.984	0.250	0.375
Exit Mach number	1.0 - 5.9	1.0	4.1	3.5

GP73-0587-43

3.2 Model holders

The model holder shape and size were dictated by the uniform heat flux requirement of the program and by the test stream size. The PAT facility provides a circular test stream issuing from an 8 in. (20.3 cm) diam exit, 15 deg (0.26 rad) half-angle conical nozzle. The jet diameter at the nozzle exit is reduced by the calculated boundary layer displacement thickness according to Ref. 2:

$$\frac{\delta}{s} = c \left(\frac{\rho_r V s}{\mu_r} \right)^{-0.3} \tag{1}$$

For a typical anticipated test condition of 1 atm (1.0133×10^5 N/m^2) stagnation pressure and 2500 Btu/lb (5.8×10^6 J/kg) enthalpy with a 0.55 in. (1.4 cm) diam throat, the calculated boundary layer displacement thickness is 0.66 in. (1.7 cm). This agrees closely with visual observation and photographs of the jet.

The test stream continues to expand after leaving the conical nozzle until it is reflected by the jet boundary or turned by a shock wave. The location of the jet boundary is dictated primarily by the background pressure. The minimum background pressure is determined by the vacuum system pumping characteristics and the total air flow rate in the test stream. Normally the PAT facility background pressure can be adjusted with a bleed valve to properly expand the flow in the 8 in. (20.3 cm) diam exit nozzle and maintain the exit jet boundary diameter for several inches downstream.

Testing experience has shown that it is not prudent to exceed the local diameter of the exit Mach cone when sizing a model. Models larger than the Mach cone diameter experience non-uniform flow conditions and undesirable edge effects resulting from bow shock-jet boundary interactions. The maximum model radius at a given axial position is approximately:

$$R_{max} = R_1 - x \tan \left(\sin^{-1} \frac{1}{M} \right),$$

or $$\tag{2}$$

$$R_{max} = R_{ex} - \delta - x \tan \left(\sin^{-1} \frac{1}{M} \right).$$

Models smaller than this are immersed in the undisturbed flow emerging from the nozzle and normally yield uniform pressure and heating profiles.

The expected operating conditions for testing the metallic specimens were initially 1 atm (1.0133×10^5 N/m^2) stagnation pressure and 2500 Btu/lb (5.8×10^6 J/kg) enthalpy. Correcting for the boundary layer displacement thickness and assuming frozen, one-dimensional inviscid core flow, the exit Mach number for these conditions was calculated to be 5.18. During the calibration tests it was necessary to increase the nozzle throat size to 1.00 in. (2.54 cm) to obtain the proper test conditions. This resulted in an exit Mach number of 4.6.

For the purpose of model design, the exit Mach cone was assumed to originate at the edge of the calculated and observed boundary layer. An axial position of 3 in. (7.6 cm) was assumed for the model location. The calibration phase dictated the final axial position selected [4 in. (10.2 cm)].

Using Eq. (2), the maximum model radius was:

$$R_{max} = 4.0 - 0.66 - 3 \tan \left[\sin^{-1} \left(\frac{1}{5.18} \right) \right]$$

$$= 2.75 \text{ in. (6.98 cm)}.$$

Thus, the maximum diameter of 5.5 in. (14.0 cm) was chosen to allow testing the largest possible sample.

In addition to the physical limitations, the following items were also considered in the model holder design.

- Ease of model changes,
- Interchangeable parts,

- Minimum instrumentation changes,
- Use of existing model actuator and support arms, and
- Close proximity of pressure transducers to the sensing point for best response.

Figure 3 depicts the model holder used in this program. The main body was a 2 in. (5 cm) long, 5.5 in. (14 cm) diam, water-cooled copper cylinder with a 4.125 in. x 4.125 in. x 1.5 in. (10.5 x 10.5 x 3.8 cm) pocket in the front surface. The pocket corners were chamfered 0.685 in. (1.74 cm) at a 45 deg (0.79 rad) angle to keep the entire sample within the uniformly heated region of the holder surface.

A 4 in. x 4 in. (10.2 x 10.2 cm) sample (with chamfered corners) was held in place by four conical tipped screws, each at the midpoint of the model sides (later eight were used; see Section 3.4). The midpoint location allowed thermal expansion away from the retainer pin. Each conical point protruded from the model holder through a 0.125 in. (0.318 cm) diam hole into a 0.25 in. x 0.25 in. (0.635 x 0.635 cm) tab on the model. The screw travel was slanted at the cone half-angle so the bottom edge of the conical tip remained parallel to the sample surface yet moved perpendicular to the surface for sample height adjustment. A 0.0625 in. (0.159 cm) gap (initially filled with Fiberfrax) existed between the cold sample edge and model holder. Allowance for thermal expansion was based on that of TD-NiCr at 2200°F (1478 K) and it was assumed that all of the metallic materials to be tested had comparable thermal expansion coefficients. Each sample was backed by a 1.5 in. (3.8 cm) thick Silfrax insulator.

A single inlet and outlet routed cooling water to the model holder walls. The milled cooling passage ensured high velocity cooling water adjacent to the front surface except at the chamfer locations. The maximum holder temperature at these corners was calculated to be less than 120°F (322 K) with a cold wall heat flux of 25 Btu/ft^2 sec (283 kW/m^2).

Each model holder was equipped with two 0.125 in. (0.318 cm) diam calorimeters and two 0.065 in. (0.165 cm) diam pressure taps located at the edge of the sample pocket, 2.187 in. (5.55 cm) from the center of the holder as shown in Fig. 3. These sensors allowed independent continuous monitoring of the cold wall heating rate and surface pressure during model tests.

Five tapped holes were provided in the holder pocket base for retaining the spring-loaded thermocouples that were initially used to monitor the sample temperature. These holes were at the sample center and at the center of each quadrant.

Four removable metal plugs were provided for mounting the back-up insulator thermocouples. Interchangeable plugs with attached thermocouples allowed rapid changeover.

Each of the two model holders was bolted to a combination sting and terminal housing that positioned the sample in the test stream and provided a local terminal for all instrumentation. The terminal housing and model holder sting (Fig. 3) evolved from the combined requirements to maintain the model holder rigid in the test stream and to provide the simplicity of a local instrumentation terminal. This apparatus was basically a copper box with a circular front plate and an exit conduit. The front plate bolted directly to the model holder and had a 2.5 x 3.0 in. (6.35 x 7.62 cm) opening for protruding thermocouple components, wiring and pressure tubes.

The insulated instrumentation leads were routed to one of the 44 spring-loaded terminal receptacles in the housing. Wiring from the underside of the terminal receptacles was routed either down the axis of the water-cooled model actuator arm or through a water-cooled conduit in back of the arm. Pressure tubing was routed through the conduit to the transducer housing mounted on the model actuator hub.
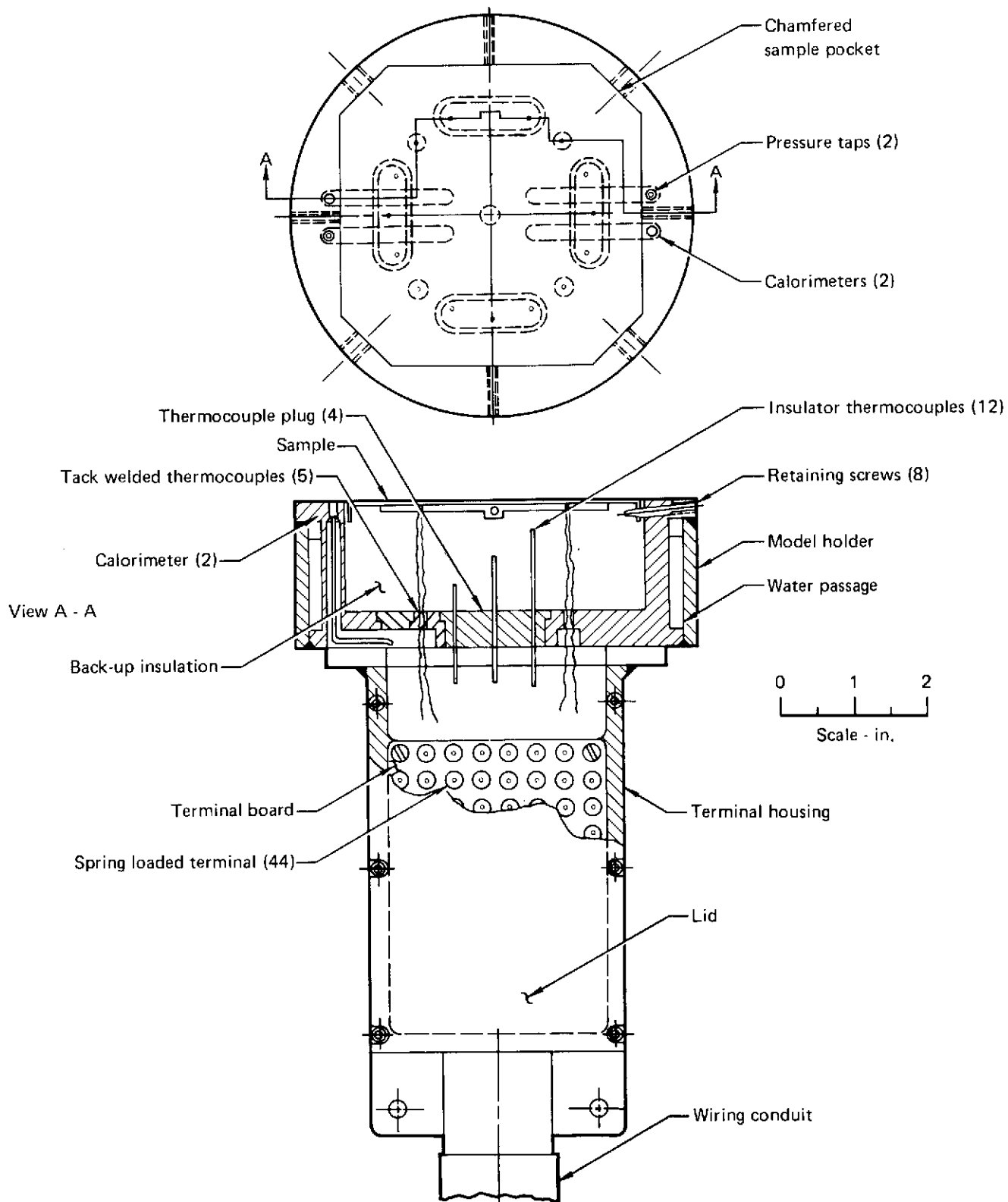
Chamfered sample pocket

Pressure taps (2)

Calorimeters (2)

Thermocouple plug (4)

Sample

Tack welded thermocouples (5)

Calorimeter (2)

View A - A

Back-up insulation

Insulator thermocouples (12)

Retaining screws (8)

Model holder

Water passage

0   1   2

Scale - in.

Terminal board

Spring loaded terminal (44)

Terminal housing

Lid

Wiring conduit

Fig. 3   Model holder and terminal housing sting
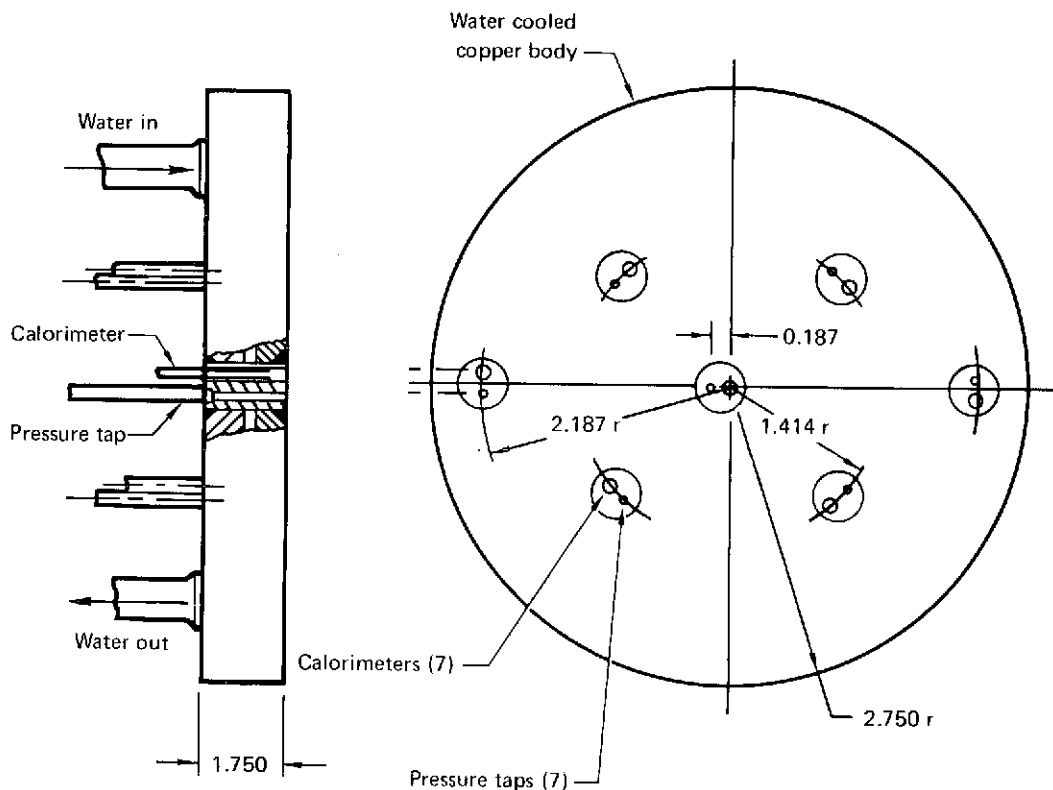
GP73-0587-3

MCDONNELL DOUGLAS

The housing-sting was not directly water-cooled, but, was in intimate contact with the water-cooled model holder and actuator arm and was shielded from the test stream by the 5.5 in. (14 cm) diam model holder.

3.3 Calibration module

Figure 4 depicts the calibration module used to define the local stream characteristics of the test sample. The 5.5 in. (14 cm) o.d. was identical to the model holder. The main body was 0.75 in. (1.9 cm) thick water-cooled copper.

Seven instrumentation plugs were located at positions corresponding to the model backface thermocouples and to the calorimeters on the

sample holder. Each water-cooled plug contained a Hy-Cal Model C-119 calorimeter and a 0.065 in. (0.165 cm) diam pressure tap. The calorimeters were quoted by the manufacturer to have an accuracy of $\pm 2\%$ full range (0-80 Btu/ft^2 sec or 0-9.1 x 10^5 W/m^2). These sensors were chosen to meet the original requirements of the contract which called for testing several types of materials at conditions predicted to require heating rates from 13 to 79 Btu/ft^2 sec (1.5 x 10^5 to 9.0 x 10^5 W/m^2). The sensors in the plugs that corresponded to the model quadrant centers were all on a 1.4 in. (3.6 cm) radius. The center plug located the calorimeter exactly on center and the pressure tap slightly off center. The two outer plugs oriented the calorimeters and pressure taps on a 2.187 in. (5.55 cm) radius at locations corresponding to the sensors on the model holders.

Fig. 4 Calibration model

All dimensions in inches

GP73-0587-4

MCDONNELL DOUGLAS

A transient calibration module was also used later in the program after encountering durability problems with the Hy-Cal sensors. The outside dimensions and heat flux sensor locations were identical to the steady-state calibration module. Seven 0.125 in. (0.138 cm) diam, 0.125 in. (0.318 cm) thick copper slugs were used as sensors. Each sensor was insulated from the holder by a 0.125 in. (0.318 cm) thick jacket of Sauereisen having a thermal conductivity of 2.84 Btu/hr/ft°F (0.492 W/mK). To provide this insulation gap around each heat flux sensor, the pressure ports were moved on the same radii 0.062 in. (0.157 cm) from their positions on the steady-state, water-cooled module.

All tubing and instrumentation wiring was routed through a sting-terminal housing as was done with the model holders. Each pressure tube was routed to a separate transducer.

Rapid response by the pressure sensors was achieved by minimizing the volume between the sensing point and the sensing element. Minimum volume was achieved in the sensing lines by housing 11 pressure transducers directly on the model actuator hub. Twelve in. (30.5 cm) long, 0.065 in. (0.165 cm) i.d. tubing connected each pressure tap and transducer. All components rotated together during indexing of the model actuator.

Figure 5 depicts the transducer housing used. An 8 in. (20.3 cm) diam copper canister 8 in.
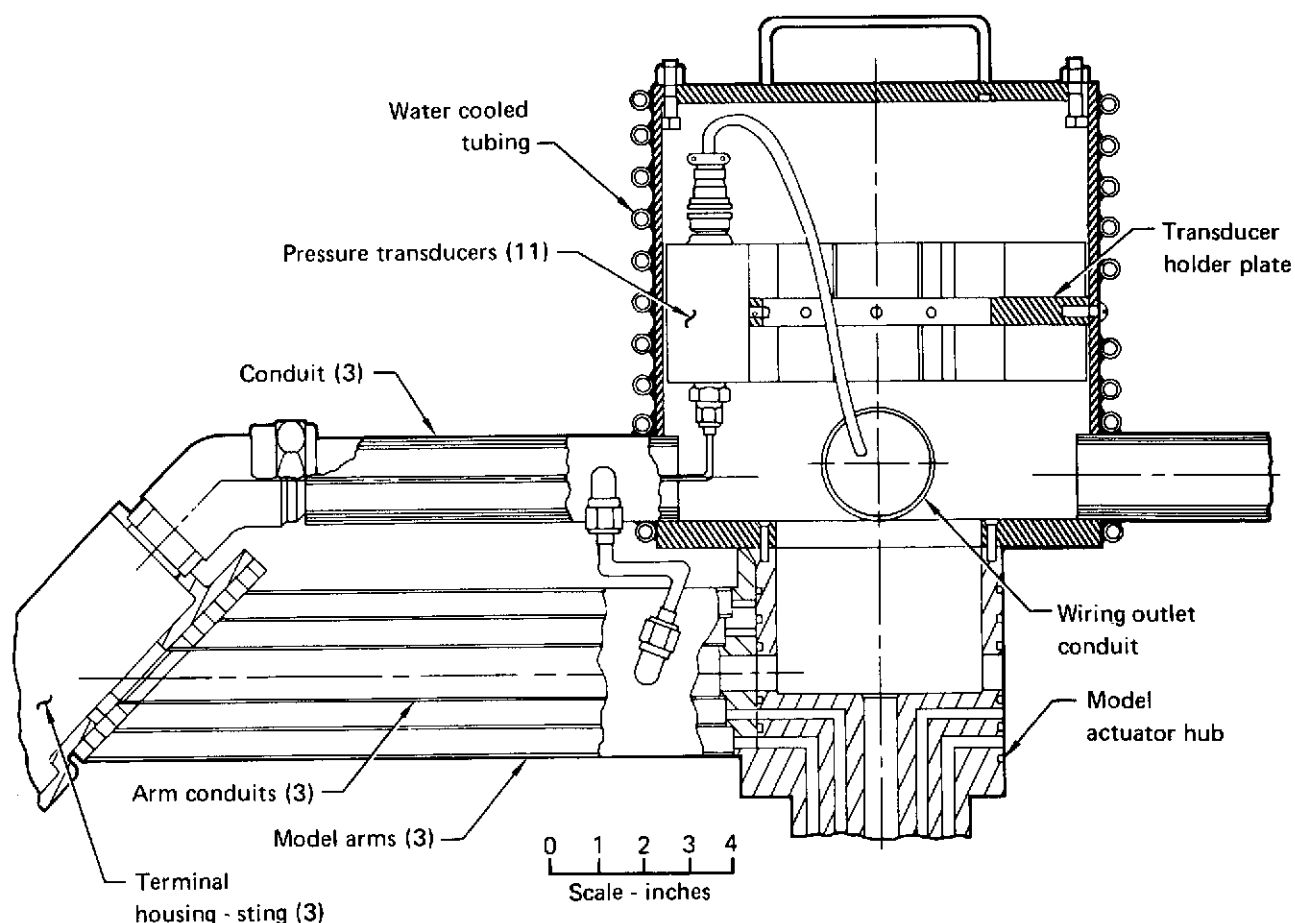

Fig. 5 Pressure transducer housing

GP73-0687-6

(20.3 cm) high was wrapped with water-cooled copper tubing and fitted with a lid and bottom plate. An annular ring retained the 11 transducers near the inside wall. Transducer connections were made as shown in Fig. 5 with the leads routed out through a 2 in. (5 cm) diam water-cooled conduit. Three water-cooled conduits protected the pressure lines coming from the calibration module and the two model holders. The bottom plate on the canister opened into the existing model actuator hub allowing instrumentation wiring to be routed through the water-cooled model holder arms as well as the auxiliary conduits.

3.4 Models

Design emphasis was placed primarily on meeting the requirements for testing metallics since the majority of the tests were to be on this type of material. Maximizing the sample size was important in order to obtain tensile test bars from the metallic samples following the thermal cycles. Contact between the sample and the holder was minimized to eliminate heat conduction losses from the sides. The size limitations are discussed in Section 3.2.

The initial metallic sample design used is shown in Fig. 6. The sample was 4 x 4 in. (10.2 x 10.2 cm) with 0.640 in. (1.63 cm) x 45 deg corner chamfers to preserve heat flux uniformity. The sample thickness (t) was of the order of 0.010 to 0.016 in. (0.025 to 0.041 cm). The four sides were bent down at the edges to prevent gross surface distortion during test. The bend radius (R_b) on the edge varied with the material from 5t to 10t. The side height (W) was approximately 0.10 in. (0.25 cm). Each side had a 0.25 in. (0.64 cm) wide, 0.25 in. (0.64 cm) long hold-down tab with a 0.125 in. (0.318 cm) diam hole to accommodate the retaining screws.
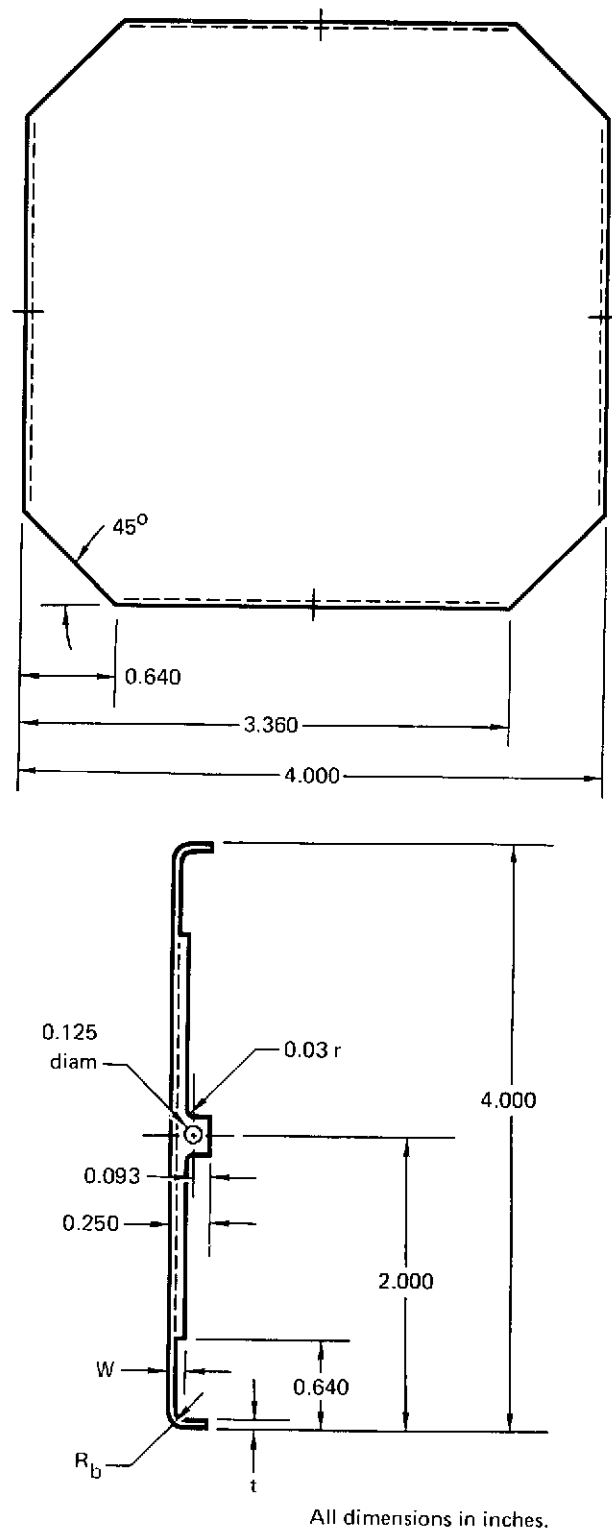

Fig. 6 Metallic sample

GP73-0587-6

The first samples were made from 0.020 in. (0.050 cm) and 0.010 in. (0.025 cm) thick TD-NiCr material acquired by MDRL and were used during the preliminary runs to help establish the required arc heater operating conditions. These samples also were used to check the MDRL designed probe and spring-loaded thermocouples and the pyrometer automatic positioning system. Two types of samples were fabricated, with and without a bend radius on the chamfered corners. It was determined during these preliminary runs that the bend radius was necessary on the chamfered corners as well as the sample edges in order to maintain a flat surface during testing.

It was found in later tests that less sample distortion was experienced while testing the higher temperature [2200°F (1478 K)] samples than when testing the moderate [2000°F (1367 K)] temperature samples. It was, therefore, anticipated that more difficulty might be experienced in maintaining a flat sample at 1800°F (1256 K). As a result, the samples to be tested at this condition were fabricated with eight hold-down tabs rather than four. In addition to a tab at the midpoint of each sample edge, a tab was placed at the midpoint of each chamfered corner. This technique worked well with no apparent adverse effects.

3.5 Instrumentation

The PAT facility was fully instrumented to provide permanent signal recordings as well as instantaneous visual readouts during the tests. All the data were continuously recorded by the Research Data Acquisition System (RDAS) on 7 track, 556 bps (218.9 bpcm) IBM compatible magnetic tape at a recording rate of 10 channels/sec.

3.5.1 Facility

The instrumentation required to define the arc heater operating conditions involved the measure-

ment of pressures for primary and secondary air flow rates, chamber pressure, two water coolant temperature differentials (ΔT's), two water coolant flow rates, arc voltage and arc current. These values were then used to calculate the test stream bulk enthalpy. The calibration module was used to measure heat flux and pressure in the resultant characteristic test stream.

A summary of the instruments used for these measurements and probable system accuracies are presented in Table 2. The full-scale measuring capability of each instrument is also presented.

3.5.2 Model

Measurement of the model temperatures was accomplished using three different techniques. Surface temperature measurements were made using a Thermodot Model TD-9H infrared pyrometer. This technique is described further in Section 3.5.3. Another non-contact technique utilized an AGA Thermovision Model 680 infrared scanning camera (see Section 3.5.4). A third non-contact measurement technique utilizing a two-color pyrometer was attempted, but the instrument exhibited erratic behavior. After several attempts at shielding the sensor from extraneous radiation failed, the use of this system was eliminated.

The only contact method of measuring the temperatures of the metallic samples was by using Pt-Pt 10% Rh thermocouples. The initial attempt utilized Baldwin-Lima-Hamilton (BLH) spring-loaded thermocouples as shown in Fig. 7. This basic thermocouple design was later modified to provide a larger movement in the thermocouple travel. However, this design modification was not adequate since the thermocouple sheath did not have sufficient strength.

A new spring-loaded thermocouple (Fig. 8) was then designed by MDRL and fabricated from 10 mil diam Pt-Pt 10% Rh standard grade thermocouple wire. A thermocouple welder was used to provide a small bead at the junction of each thermocouple. The wires from the bead were

Table 2 Instrumentation

| Parameter	Instrument	Recorder	Range	System accuracy
Arc heater				
Arc pressure	Statham type PA220TC-50-350	RDAS*	0-50 psia	±0.50%
Arc voltage	MDC voltage divider	RDAS	0-2000 V	±0.35%
Arc current	GE Model JDC-1 current transformer	RDAS	0-1000 A	±0.75%
Primary air flow	MDC sonic flowmeter	RDAS	10^{-3} - 10^{-1} lb/sec	±1%
Secondary air flow	MDC sonic flowmeter	RDAS	10^{-3} - 10^{-1} lb/sec	±1%
Arc heater ΔT	Delta T's	RDAS	0-100°F	±0.3%
Water flow rates	Turbine meters	RDAS	0-70 gpm	±0.55%
Metallics				
Backface temperature	BLH No. SLPR10-WS-125 thermocouple	RDAS	0-3000°F	±0.55%
	Pt-Pt/10% Rh tack-welded thermocouple	RDAS	0-3000°F	±0.55%
Surface temperature	Thermodot Model TD-9H pyrometer	RDAS	1840-2720°F	±3% of range span
	AGA thermovision model 680 camera	Polaroid	0-3600°F	±0.36°F max resolution
Surface emissivity	MDC emissometer	—	0-1	±4%
Insulation temperature	Pt-Pt/10% Rh thermo-couples	RDAS	0-3000°F	±0.55%
Heat flux	Hy-Cal model C-119 calorimeter	RDAS	0-80 Btu/ft^{2}sec	±2%
Impact pressure	CEC type 4-353-0001	RDAS	0-0.5 psia	±0.35%
Weight	Voland 220 analytical balance	Hand	0-220 g	±0.001 g
Size	Starrett micrometer	Hand	0.001-3.0 in.	±0.0001 in.
Calibration model				
Heat flux (7)	Hy-Cal model C-119 calorimeter	RDAS	0-80 Btu/ft^{2}sec	±2%
	MDC transient calorimeter	Oscillograph	—	—
Impact pressure (7)	CEC type 4-353-0001	RDAS	0-0.5 psia	±0.35%

*Research data acquisition system

GP73-0587-44
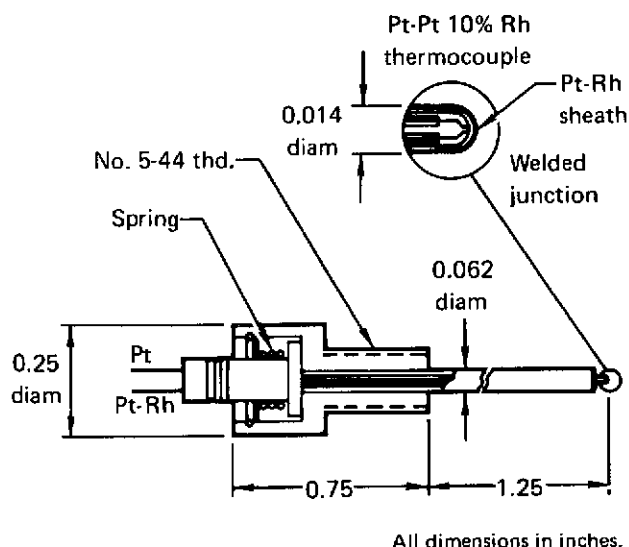
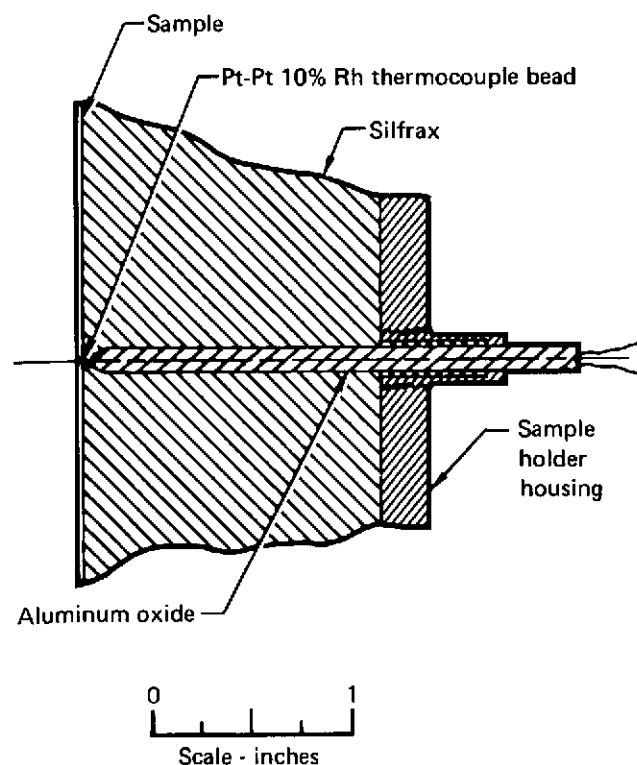Fig. 7 Spring-loaded thermocouple for sample backface

GP73-0587-7

Fig. 8 MDRL spring-loaded thermocouple

GP73-0587-8

routed through small double bore aluminum oxide tubing. A ring was bonded with ceramic cement near one end of the aluminum oxide tubing to provide a support for the spring. The spring holder-thermocouple support was threaded externally to fit a threaded hole in the model holder body. Adjustment of this threaded support combined with varying the length of the spring provided a spring-loaded axial movement of approximately 0.25 in. (0.64 cm) for each thermocouple.

This spring-loaded thermocouple design still produced significant temperature discrepancies when compared with the pyrometer measurements. The decision was then made to establish a test set-up in which the temperatures measured by the various spring-loaded thermocouple designs could be compared with tack-welded thermocouple measurements. The results of these tests (Section 6.1) prompted the decision to test all remaining samples using tack-welded thermocouples at five locations on the metallic samples. These locations were on the center of the model and the center of each of the four model quadrants.

It was originally planned to use BLH miniature probe thermocouples to measure the back-up insulation temperatures. However, these 0.014 in. (0.036 cm) diam probes were found to be too fragile for this application. As a result, a probe thermocouple was designed and fabricated by MDRL using 0.010 in. (0.025 cm) diam Pt-Pt 10% Rh thermocouple wire routed through 0.063 in. (0.160 cm) diam double bore aluminum oxide tubing. This design had the required strength and thus was used for the test program.

After it had been initially determined that the in-depth position was critical to achieve good temperature agreement, the back-up insulation thermocouples were precisely positioned using a special test fixture. The in-depth thermocouples were all located on a radius of 1.414 in. (3.592 cm) at three depths of 0.375, 0.750, and 1.125 in. (0.952, 1.905, and 2.858 cm). The 12 in-depth thermocouples and 4 of the surface thermocouples

were equally spaced on the 1.414 in. (3.592 cm) radius (Fig. 3).

3.5.3 Pyrometer

A Thermodot Model TD-9H automatic optical pyrometer designed to measure temperatures between 1840 and 8300°F (1278 and 4867 K) using three ranges was used to radiometrically measure the sample surface temperature. It had a 1.5 in. (3.8 cm) diam f/6 lens. The detector was a silicon pn junction photovoltaic sensor sampling monochromatically at 0.8 μm.

The pyrometer was calibrated by the McDonnell Aircraft Company (MCAIR) Bureau of Standards using a Pyrometer Instrument Company 95M4376 optical pyrometer as a standard. The calibration accuracy was ±3% of range span [1840 - 2720°F (1278 - 1767 K)].

The pyrometer viewed the sample through a General Electric 125 fused quartz window 0.5 in. (1.27 cm) thick. The sighting angle was 21.2 deg (0.37 rad). Cold air was uniformly injected around the viewing port inside the vacuum tank to prevent particle contamination of the window. The pyrometer lens was 3 in. (7.6 cm) from the window and 50 in. (1.3 m) from the test sample.

Pyrometer sightings were sequenced automatically by the two-dimensional slide positioning system. The pyrometer automatic positioning system provided two pyrometer scans of five points each (coinciding with sample backface thermocouple locations) on the model surface during each 600 sec test cycle. A sixth position was used as a reference to check system sample to sample repeatability. One of the pressure ports on the model holder was used as this reference position. Outputs from potentiometers on the positioning system drive motors were recorded on the data system so a temperature-time-position correlation could be made.

Figures 9 and 10 illustrate the pyrometer arrangement used on this program. The basic two-
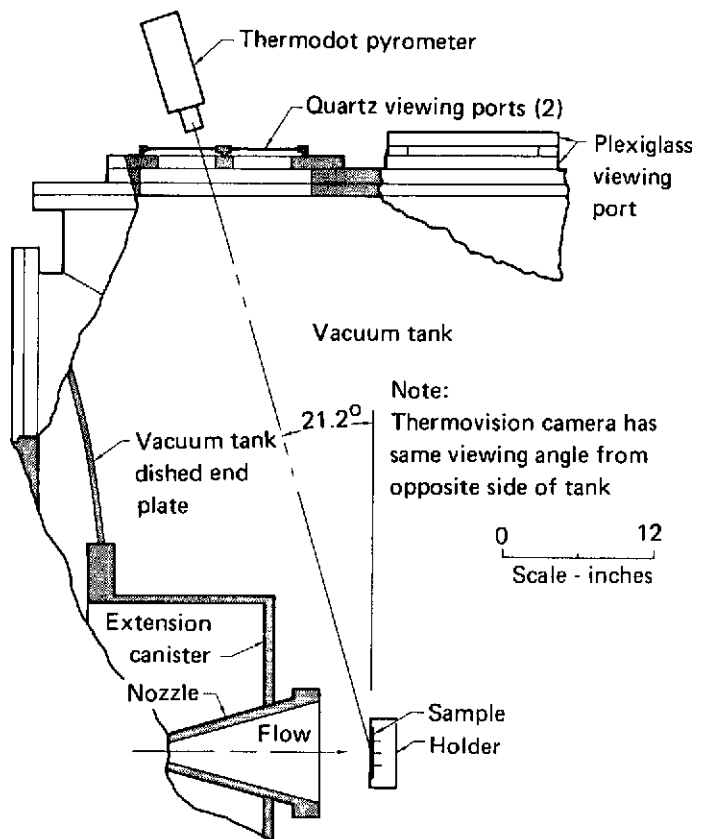

Fig. 9 Pyrometer viewing angle

GP73-0587-9

dimensional positioning device was a Gilman Model L6-12-4/L6-12-4 lead compound, which had a 4 x 4 in. (10 x 10 cm) travel and an accuracy of ±0.001 in. (±0.0025 cm); the compounds were driven by small 28 V motors. A precision Helipot Model 7603 potentiometer tracked the position of each compound slide and gave a continuous position output. It also was an integral part of the position feedback for sequential sampling of five locations on the model.

3.5.4 IR scanning equipment

An AGA Model 680 Thermovision System was positioned in a location similar to that of the pyrometer but on the opposite side of the vacuum tank. This unit continuously viewed each sample through a CaF_2 window (initially fused quartz) to determine the model surface temperature distribution.
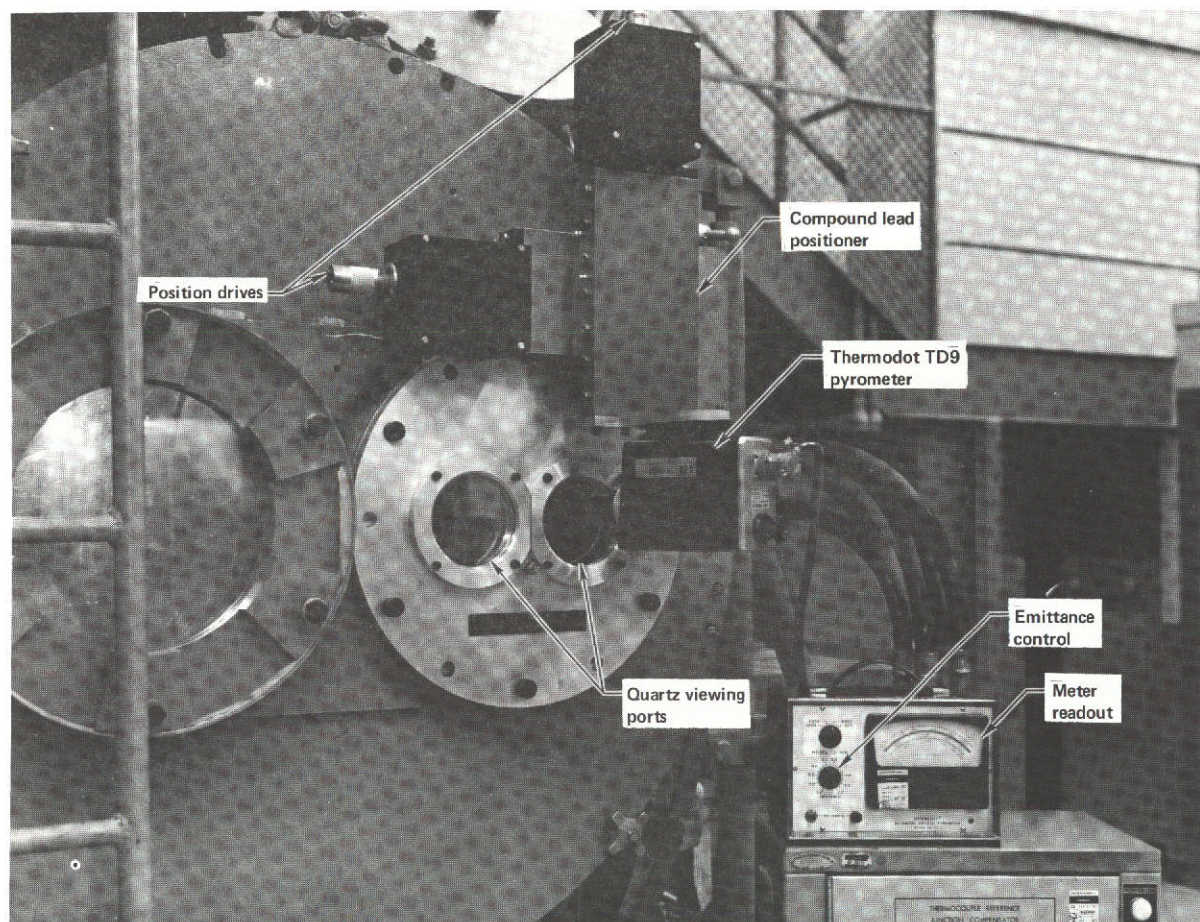
MCDONNELL DOUGLAS

Fig. 10 Pyrometer positioning system

The systems consists of a camera unit containing the liquid nitrogen cooled infrared detector, optical/mechanical scanner, video signal amplifiers, and the CRT display to view the thermogram.

The IR scanner in the camera unit consists of two rotating (vertical and horizontal) scanning prisms, two prism-drive motors, magnetic position-sensing heads, and a collimating lens. A virtual image is formed by the front lens of the camera on a plane within the first prism. The image is scanned vertically by rotation of the prism about its horizontal axis. This results in a horizontal, virtual line-image being formed within the second scanning prism. The line-image is then scanned horizontally in turn by rotation of the second prism about its vertical axis.

Each of the two scanning prisms is furnished with a positional pick-off ring having small triggering strips of magnetic material placed edge-on in relation to the position of each prism flat. As the prisms rotate, the triggering strips pass in front of the magnetic pick-up heads, producing electrical synchronization pulses. These pulses are used in the display unit for triggering the horizontal and vertical display sweeps to reproduce the camera scanning pattern on the CRT.

The radiant flux from the scanner impinging on the detector generates an electrical voltage signal across the terminals of the detector. The amplitude of the signal varies according to the point-by-point temperature variations along the surface of the object as it is being scanned by the

camera. The signal derived from the camera unit is amplified and used to modulate the intensity of the CRT electron beam in the display unit. The electron beam sweeps across the screen of the monitor tube in synchronism with the camera scanning-optics, under control of the trigger pulses derived from the camera unit. This produces on the display screen a thermal distribution of the object being scanned by the camera unit.

A selected amount of the infrared radiation focused on the detector in the camera unit can be marked electronically to produce isothermal contours on the display screen. Whenever the detector video signal level corresponds to the arbitrary isothermal level selected by the operator, the electron beam of the CRT is automatically switched to maximum intensity. This causes all areas in the thermal picture having the selected temperature level to be delineated in saturated

white. The isotherms thus produced can be used to measure the exact amount of temperature variation existing between details on the thermal image of an object.

3.5.5 Emissometer

Total normal emittance measurements were made on representative metallic strip samples using a MDC-developed high temperature emissometer.

An optical diagram is shown in Fig. 11. There are three sources of input radiation to the thermopile detector: radiation from an induction-heated inconel blackbody for calibrating the emissometer (effective emittance > 0.995); radiation from a strip of oxidized DS-NiCr used to monitor contamination of the potassium bromide infrared window mounted on the vacuum chamber; and radiation from the sample of unknown emittance.

Each radiation source can be focused on the detector by the plane rotating mirror. The radiation
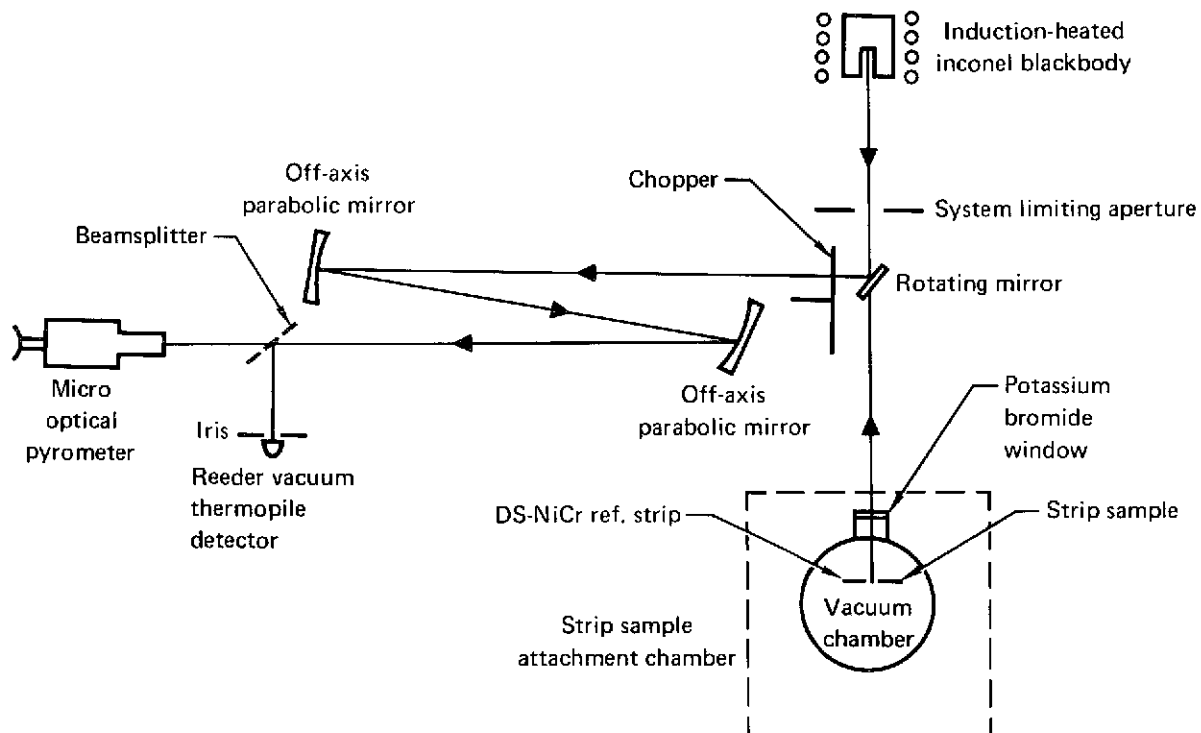

Fig. 11 High temperature emissometer with strip sample attachment

GP73-0587-11

is modulated at 13 Hz by a motor-driven chopper and transferred onto a beamsplitter by the two off-axis parabolic mirrors. The fraction of the radiation reflected by the beamsplitter is directed onto the thermopile detector (Reeder RP-5W). The transmitted part is viewed by the operator using the pyrometer. In this way precise alignment of the complete optical system can be obtained during a measurement.

The 13 Hz voltage from the thermopile is measured with a tunable microvoltmeter. Chromel-alumel thermocouples and a Leeds and Northrup 8686 millivolt potentiometer provide the required measurements of strip and blackbody temperatures. The metallic strips were heated with 6 Vac power.

At the start of a run, the emissometer is calibrated using the blackbody by recording the voltage from the thermopile detector at several temperatures. The mirror is then rotated to the DS-NiCr strip (emittance = 0.72) which is resistance heated to 1800°F. The thermopile output is recorded for comparison with subsequent

similar measurements to determine the extent of any window contamination. Finally the mirror is rotated to view the sample which is resistance heated in a 10 Torr environment to the required test temperatures (Fig. 12). The total normal emittance is calculated from Eq. (1):

$$\epsilon_{tn} = \frac{V_s - V_{bgnd}}{V_{bb} - V_{bgnd}}$$

where V_s = detector output from the sample

V_{bb} = detector output from the inconel blackbody and

V_{bgnd} = system background level.

The background level, V_{bgnd}, is measured by inserting a mirror into the optical path immediately in front of the KBr window of the sample chamber and noting the detector output.

Repeated measurements on a variety of samples indicate that the error in the absolute total normal emittance measurements was ±0.03.
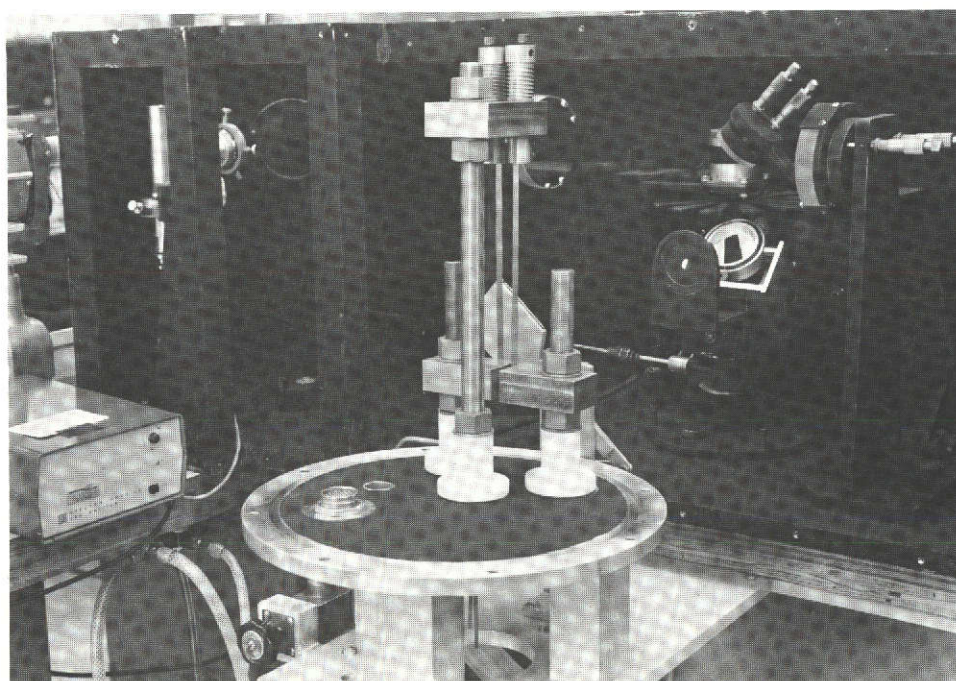

Fig. 12 Emissometer strip sample attachment chamber (housing removed)

4 Test procedure

All models were splash tested (surface perpendicular to the stream centerline) in the MDRL PAT facility with the models on the stream centerline at an axial position 4 in. (10.2 cm) downstream of the nozzle exit plane.

Three model actuator arms mounted 90 deg (1.57 rad) apart were used to support the two models and a calibration module in the vacuum test chamber. Models were mounted on arm nos. 2 and 3 with the calibration module on arm no. 1. Model surface and back-up insulation temperatures and distributions were taken continuously during each model test.

4.1 Model preparation

All materials tested in this program were superalloy metallics supplied by the NASA Lewis Research Center Materials and Structures Division. The material was shipped to the MDRL where the test models were fabricated.

The first NASA samples were fabricated from DS-NiCr and identified as DS-3 and DS-4. Identification was achieved by notching one edge radius on each sample perpendicular to the material's rolling direction. The samples were installed with the rolling direction in the horizontal plane, and the notched edge at the top.

Before installing the models in their holders, the fabricated models were cleaned thoroughly with acetone, and weighed to ± 0.0005 g on an analytical balance. Pre-test thickness measurements were recorded at nine positions (Fig. 13) on the model surface. Color 35 mm photographs were taken of the front and back surfaces of each model with the notched edge at the top of the photograph.

The models were then installed in the holders, and modifications to the back-up insulation (Silfrax) were made as required so that the model front surface would be coplanar with the holder.
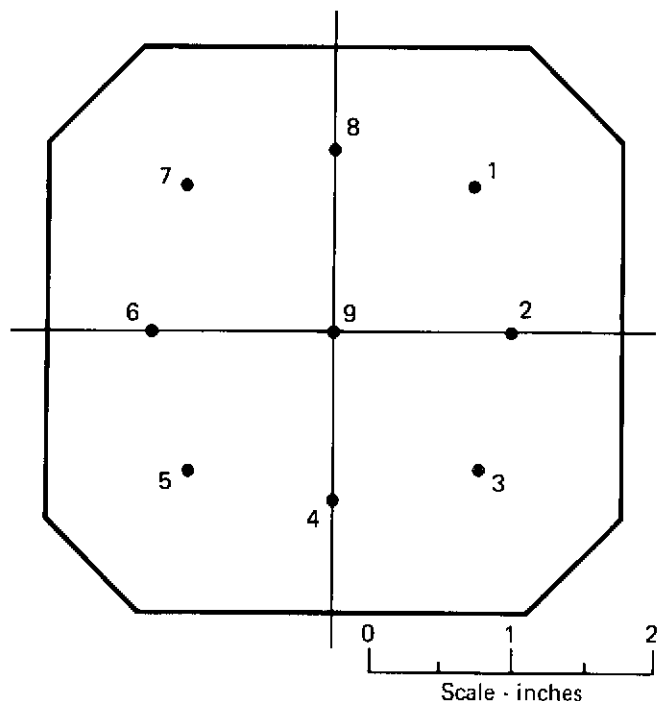

Fig. 13 Thickness measurement locations

GP73-0587-13

Narrow strips of Fiberfrax insulation were then loosely packed around the model edges to fill the expansion gap between the model and holder edge. As the models expanded during heating this gap was virtually eliminated.

The practice of filling this gap with Fiberfrax was discontinued during the early cycles on TD-5 and TD-9 with no detrimental effect, and all subsequent tests were conducted without it. In fact, the elimination of this insulation appeared to improve the model temperature distribution because of reduced material distortion. Since the Silfrax back-up insulation filled the entire sample holder cavity with the exception of the shallow gap around the perimeter of the sample, there was no flow around the sample backface.

After initial tests were conducted and it was concluded that spring-loaded thermocouples consistently measured lower than true temperatures, the use of tack-welded thermocouples was initiated with cycle 41 on model DS-3 and cycle 42 on model DS-4. To facilitate attachment of these thermocouples, the model back surface was lightly sanded in the region of attachment and cleaned with acetone as were the thermocouple wires. An additional wire was attached to the center of the sample and used as a ground wire to minimize instrumentation noise.

On all subsequent models a weight was obtained following surface sanding and cleaning, and an additional weight was obtained after thermocouple attachment to the cleaned surface.

4.2 Calibration

Prior to conducting the material evaluation tests, several PAT facility runs were made to establish the arc heater configuration and operating conditions necessary to produce a uniform heating distribution at sample temperatures of 1800, 2000 and 2200°F (1256, 1367 and 1478 K). Parameters that were varied during these runs included the arc current, primary gas flow rate, secondary gas flow rate, nozzle throat size, and model axial position. Heat flux and pressure distributions were measured for each operating condition using the water-cooled calibration module. Initially, the gold-plated calorimeter sensors were cleaned with dilute nitric acid prior to each run, while the copper calibration module front face was cleaned with dilute acetic acid. However, comparison of heat flux measurements made with both cleaned and uncleaned sensors for the same test conditions showed no appreciable difference. The frequent cleaning procedure therefore was abandoned as it appeared that the delicate sensor surfaces were being damaged. In fact, after approximately 400 min of arc jet exposure and 25-30 cleanings it was necessary to replace two of the sensors on the calibration module.

The final facility configuration, which provided all three test conditions by simply varying the arc current and air flow rates, included the following: a 1.0 in. (2.54 cm) diam nozzle throat which yielded a Mach 4.6 test stream at the 8 in. (20.3 cm) diam exit of the 15 deg (0.26 rad) half-angle conical nozzle; 80% silver - 20% copper electrodes; and a model axial position of 4 in. (10.2 cm) from the nozzle exit plane.

To assure test environment uniformity and repeatability, the calibration module was inserted into the test stream several times while making the required number of thermal cycles on each set of samples. The Hy-Cal heat flux sensors did not have the durability expected. After completing only 15% of the test program, a total of five sensors on the calibration module had been replaced. As a result, it was decided to modify the calibration module to replace the Hy-Cal sensors with transient slug calorimeters (see Section 3.3).

Measurements with the new calibration module utilizing transient calorimeters indicated that the heat flux values were 3-4 Btu/ft^2 sec (3.4-4.5 x 10^4 W/m^2) higher than the Hy-Cal measured values at

the same arc heater operating condition. However, the ±2% full range accuracy (Section 3.3) quoted by the manufacturer, Hy-Cal Engineering, could account for much of this discrepancy.

A thin coating of dupont Teflon-S was applied to the transient heat flux sensors prior to one run to provide non-catalytic surfaces. Comparison of the data from this run with data obtained at similar conditions with uncoated sensors showed a ratio of approximately 0.8.

The heat flux and pressure calibration data obtained while testing each set of samples are shown in Figs. A-1 through A-11 in Appendix A, Volume II, of this report. Typical data for two different test conditions are shown in Figs. 14 and 15 of this volume. Each data point shown is an average of several runs. The measured profiles show a test stream uniformity generally within ±10% for the heat flux and ±5% for the pressure.

Fig. 14 Heat flux and pressure calibration for samples HS-1 and HS-2 tested at 1800°F

4.3 Testing

The test procedure was as follows:

1. The arc heater was started and stabilized at the required test stream condition with no model in the stream.

2. The calibration module on arm no. 1 was inserted into the stream, and fine adjustments were made in the arc heater controls to achieve the desired heating rate and impact pressure. Beginning with TY-1 and TY-2 model tests, transient sensors were used to measure the test stream conditions and no adjustments were made on the arc heater controls while the calibration module was in the test stream.

3. As the calibration module left the test stream, arm no. 2 entered.
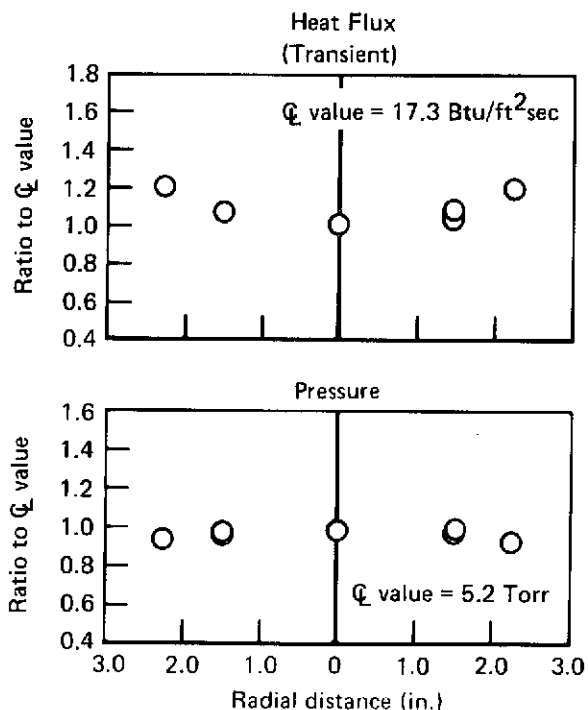

Fig. 15 Heat flux and pressure calibration for samples TD-7 and TD-8 tested at 2200°F
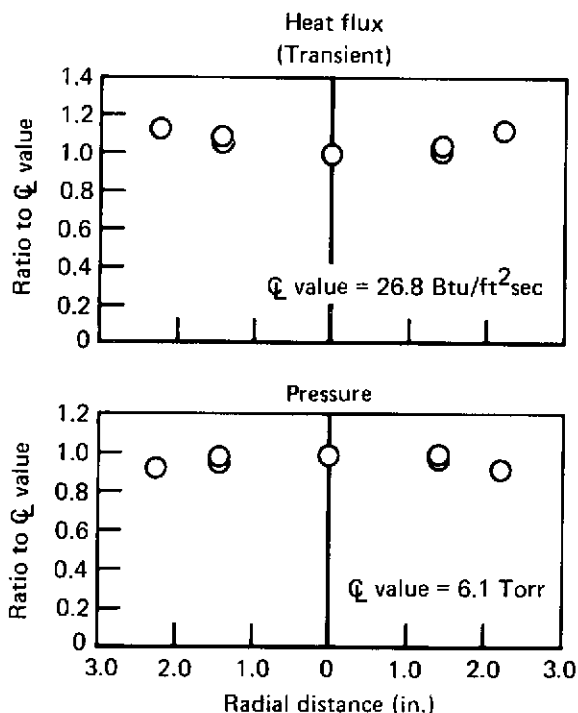
MCDONNELL DOUGLAS

4. The model on arm no. 2 was tested for the prescribed number of 10 min heating cycles with continuous monitoring of the backface temperatures (5), the Silfrax insulation temperatures (12), the model holder heating rate (2), the model holder pressure (2), and the arc heater operating parameters (9).

5. The surface temperature of each model was measured with a TD-9H pyrometer at five pre-selected points which corresponded to the five backface thermocouple attachment positions on the model. Two scans of the positions were completed during each 10 min test cycle.

6. The surface temperature distribution was determined using an AGA Model 680 Thermovision, at a frequency of one complete thermogram per cycle. Black and white Polaroid thermograms were taken on all tests through cycle 33 on models HS-1 and HS-2. Each thermogram contained five to eight isotherms. Data interpretation became more difficult on the models tested at the lowest temperature, and a camera was obtained for taking 35 mm color thermograms. These were easier to interpret and thus were used on all subsequent tests.

7. After completion of the prescribed test time, arm no. 2 was indexed out and arm no. 3 was indexed into the test stream.

8. Steps 4, 5, and 6 were repeated for this model.

9. Arm nos. 2 and 3 were alternated for the prescribed number of cycles before physical measurements were made on the models.

10. All models tested for 100 cycles were removed and photographed front and back: weight and thickness measurements were recorded after 25, 50, 75, and 100 cycles. Models tested for 50 cycles were removed for measurements after 15, 30, and 50 cycles.

11. Prior to facility shutdown, the calibration module was indexed into the test stream to check the heat flux and pressure distributions.

12. The models were reinstalled after the measurements were made and thermocouple repairs (if needed) were completed. Testing was resumed as outlined in steps 1 through 11.

13. When the required number of test cycles had been completed and final post-test measurements were made, the models were securely suspended in a small metal box (2 per box) and shipped air express to NASA Lewis Research Center.

4.4 Post-test measurements

After each model was removed from the holder, a total weight was taken and recorded with respect to the number of cycles completed. For those models instrumented with tack-welded thermocouples, this total weight included the thermocouple and ground wire weights. If any wires were broken during removal or if any had detached during testing, they were also weighed with the model. All personnel assisting in model removal wore white nylon gloves to minimize contamination of the sample surface. Special care was taken during handling of the models to prevent damage. The models were then photographed on the front and back surfaces with a 35 mm color camera.

Thickness measurements at the nine locations shown in Fig. 13 were made using a standard micrometer with an accuracy of ±0.0001 in. (2.54×10^{-4} cm). If any thermocouples required rewelding, a small area was sanded lightly and cleaned with acetone prior to tack-welding the thermocouple at its original attachment point. Before rewelding the thermocouple wires, another total weight was taken with any loose wires

included, so the weight loss that occurred during surface preparation could be determined. After reattachment of any loose wires, the total weight was again measured. The models were then care- fully reinstalled in the holders to prevent damage to the model, but some unaccountable weight losses may have occurred.

MCDONNELL DOUGLAS

5 Model tests

A total of 325 test hours were conducted on 21 metallic samples fabricated from six different superalloy materials. A typical model during test is shown in Fig. 16. The sample test order, material identification, control temperature, arc heater nominal operating conditions, and test stream conditions are given in Table 3. The enthalpy values shown are average exit values based on an arc heater energy balance. It should be noted that all arc heater parameter values listed in Table 3 are nominal since some adjustment of the arc heater current and flow rates was required during the runs to maintain the sample temperature at the desired level.

The entire test program was conducted without any arc heater electrode failures. The average electrode lifetime was approximately 75 operating hours for the cathode and 120 hours for the anode. Test stream contamination caused by electrode material loss was less than 0.02% by weight.
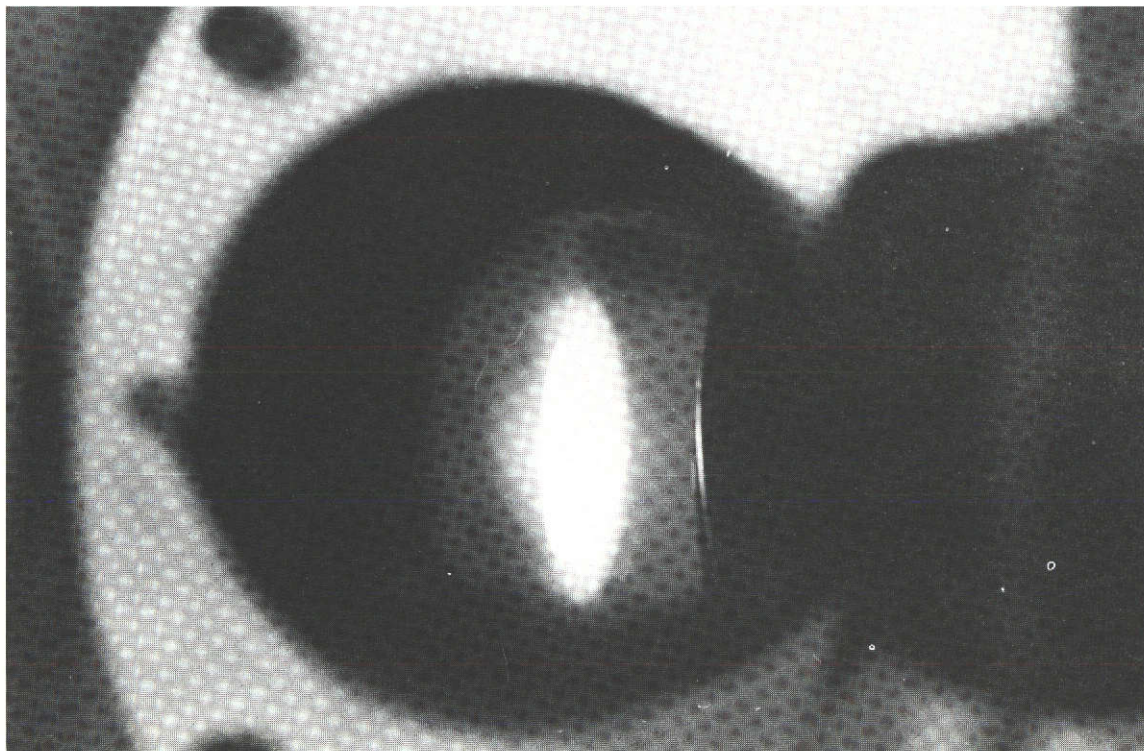

Fig. 16   Typical model during test

Table 3 Test program summary

Test No.	Sample	Material	Test temperature (°F)	E (V)	I (A)	$\dot{m}_1$ (lb/sec)	$\dot{m}_2$ (lb/sec)	Efficiency (%)	h_{ex} (Btu/lb)	$P_T'{}_\ell$ (Torr)	P_T' av (Torr)	$\dot{q}_\ell$ (Btu/ft²sec)	$\dot{q}$ Sensor used	$\dot{q}_{av}$ (Btu/ft²sec)
1.	DS-3, DS-4	DS-NiCr	2000	410 (Cycles 1-40)	640	0.015	0.010	41	4100	6.9	6.8	23.9	Hy-Cal	21.3
				410 (Cycles 41-100)	580	0.015	0.010	42	3800	6.9	6.8	18.7		17.4
2.	TD-5, TD-9	TD-NiCr	2000	390	630	0.015	0.010	39	3600	7.0	6.8	18.8		18.4
3.	TAL-1, TAL-2	TD-NiCrAl	2200	380	530	0.012	0.007	40	4000	6.0	5.7	18.7		17.7
4.	TY-1, TY-2	TD-NiCrAlY	2200	380	520	0.012	0.007	40	3900	5.9	5.7	19.4		21.4
5.	HS-1, HS-2	HS-188	1800	380	435	0.011	0.007	45	3900	5.2	5.0	17.3		18.8
6.	X-1, X-2	Hastelloy X	1800	380	390	0.012	0.007	47	3500	5.4	5.2	16.4		18.4
7.	TD-1, TD-2	TD-NiCr	1800	390	435	0.013	0.009	43	3200	5.3	5.1	16.9	Transient	18.4
8.	DS-1, DS-2	DS-NiCr	2000	400	530	0.015	0.009	41	3400	6.4	6.2	23.6		23.7
9.	TD-7, TD-8	TD-NiCr	2200	400	500	0.014	0.007	37	3300	6.1	5.9	26.8		28.4
10.	DS-5, DS-6	DS-NiCr	2000	400	550	0.015	0.009	35	3100	6.3	6.0	25.1		23.6
11.	HS-3	HS-188	2000	410	510	0.015	0.008	35	3000	6.3	6.1	25.2		23.6

Note: All samples were tested for 100 10-min cycles except samples TD-7, TD-8, and HS-3 which were tested for only 50 cycles each.

Weight and thickness measurements were made after 25, 50, 75 and 100 cycles for those samples tested for 100 cycles and after 15, 30, and 50 cycles for those samples tested for 50 cycles.

GP73-0587-45

6 Results

6.1 Physical contact temperature measurements

Platinum-platinum 10% rhodium thermocouples were used to measure 5 sample backface temperatures and 12 in-depth insulator temperatures continuously throughout each test cycle. Initially, spring-loaded backface thermocouples were used for ease of sample removal. However, it was necessary to heat the sample 4 or 5 min before even fair agreement could be reached with the pyrometer measurements. The slow response of these thermocouples compared with the pyrometer led to an investigation of their accuracy. It was suspected that contact thermal resistance and thermocouple sheath conduction were causing these errors.

As a result, an experiment was conducted to compare the outputs of various spring-loaded and tack-welded thermocouple configurations at conditions corresponding to actual sample tests. Included in the group of spring-loaded thermocouples were the BLH Model SLPR 10-WS-125 (originally planned for use on this program), an Aerotherm probe, and three MDRL designed probes. All thermocouples were Pt-Pt 10% Rh except the Aerotherm probe which was Pt-Pt 13% Rh. Five Pt-Pt 10% Rh thermocouples were tack-welded to a 0.010 in. (0.025 cm) thick, 0.25 in. (0.64 cm) wide, and 6.5 in. (16.5 cm) long,

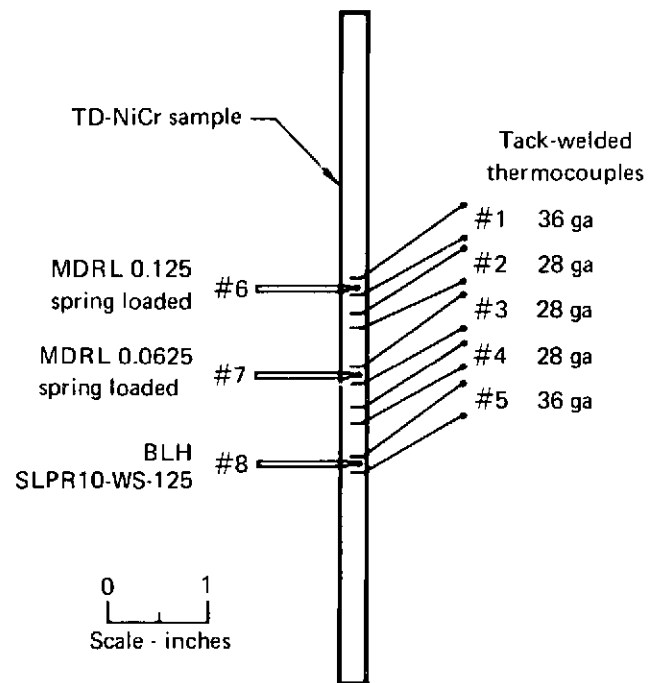TD-NiCr metallic strip as shown in Fig. 17. The outer thermocouples were 36 gauge and the inner

Fig. 17   Thermocouple locations on strip sample

GP73-0587-17

thermocouples were 28 gauge. The strip was electrically heated in a vacuum chamber as shown in Figs. 18 and 19 at a pressure of 10 Torr (1.33 x 10^3 N/m^2). Eleven temperature levels from 240 to 1620°F (388 to 1156 K) were recorded in the initial test. Four tack-welded thermocouples and the MDRL 0.125 spring-loaded probe were monitored on a Biddle-Gray 0-80.5 mV potentiometer. The BLH and MDRL 0.063 probes and the #5 tack-welded thermocouple were recorded on Honeywell Electronik 19 pen recorders. At the peak temperature, the BLH probe tip failed by bending.
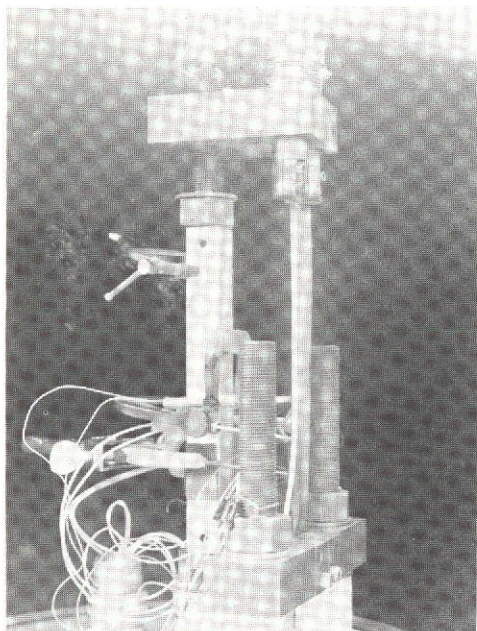
Fig. 18   Heated TD-NiCr strip sample for thermocouple calibration measurements

Additional tests were made with the output of the #3 tack-welded thermocouple on the pen recorder since it straddled the MDRL 0.063 spring-loaded probe. The strip sample temperature level as measured by the #2 tack-welded thermocouple was raised to 2200°F (1478 K) in five steps.

Other tests were made to compare the Aerotherm probe and a sharp pointed MDRL 0.063 SP spring-loaded probe (Fig. 20) with the tack-welded thermocouple outputs. An aluminum oxide sleeve was placed on one of the tack-welded thermocouples such that the sleeve was adjacent to the strip sample to determine conduction effects. During these tests the sleeve was also moved back approximately 0.125 in. (0.318 cm) from the sample for some of the test points.

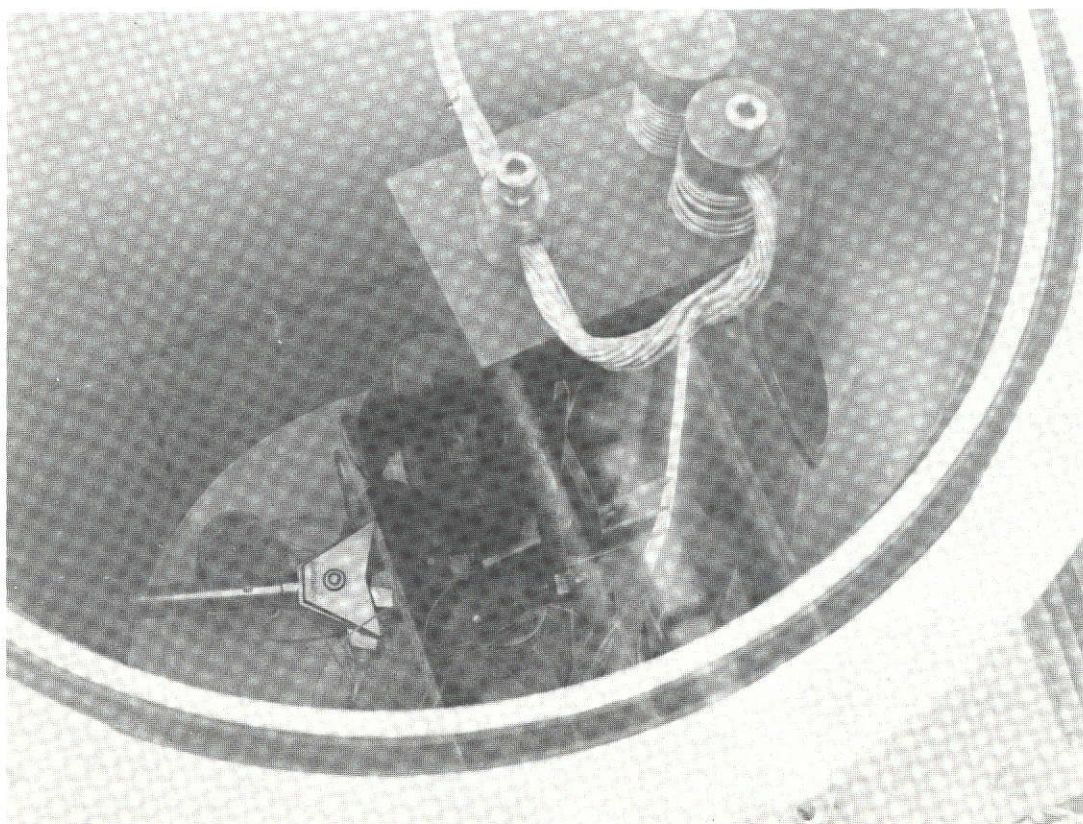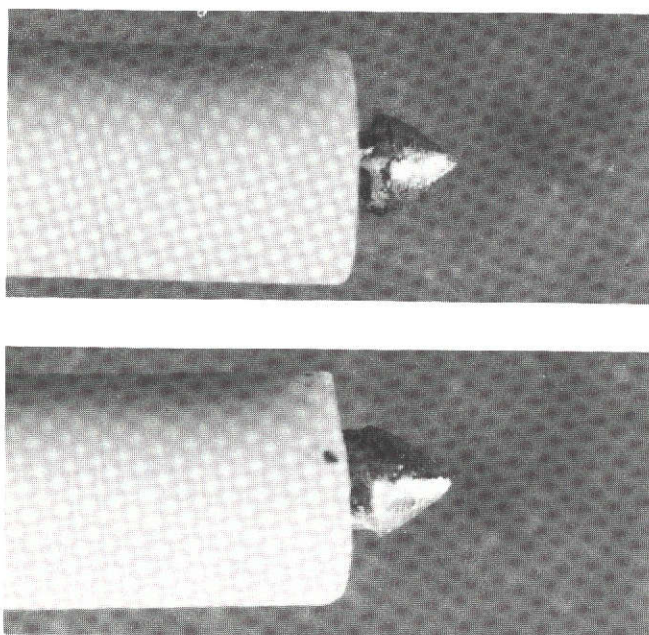Figure 21 compares all of the tack-welded thermocouple outputs with the #2 thermocouple

Fig. 19   Heated TD-NiCr strip sample for thermocouple calibration measurements

MCDONNELL DOUGLAS

Views rotated 90 deg apart

Fig. 20 Photomicrograph (24X) of MDRL 0.063 SP spring-loaded thermocouple probe

output. Differences of 60°F (33 K) were credited to the presence of local cold spots on those tack-welded thermocouples that straddled the spring-loaded ones.

Figure 22 compares all the spring-loaded probe outputs with the #2 tack-welded thermocouple output. The probe outputs are significantly lower at all temperature levels. Better agreement is achieved with the smaller probes, but differences of 300°F (167 K) existed at the temperature levels of interest, 1800 to 2200°F (1256 to 1476 K). It was concluded that conduction through the probes caused the error.

Cold spots were noted on the sample face opposite the point of contact with the probes (note mirror image in Fig. 23), but none were noted with the tack-welded thermocouples.

Significant errors were found in both the Aerotherm and the MDRL 0.063 SP probes. At the 1450°F (1061 K) level the Aerotherm probe
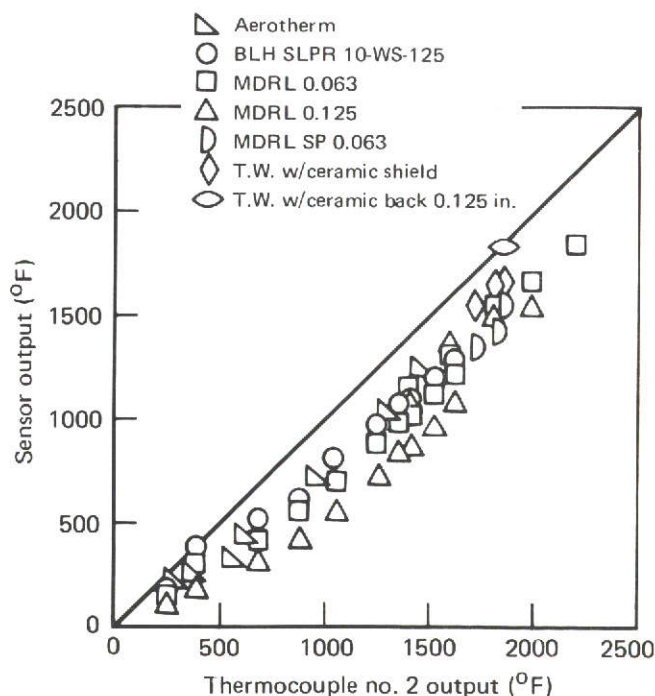

Fig. 21 Comparison of tack-welded thermocouple outputs

GP73-0587-21

Fig. 22 Comparisons of spring-loaded and tack-welded thermocouple outputs
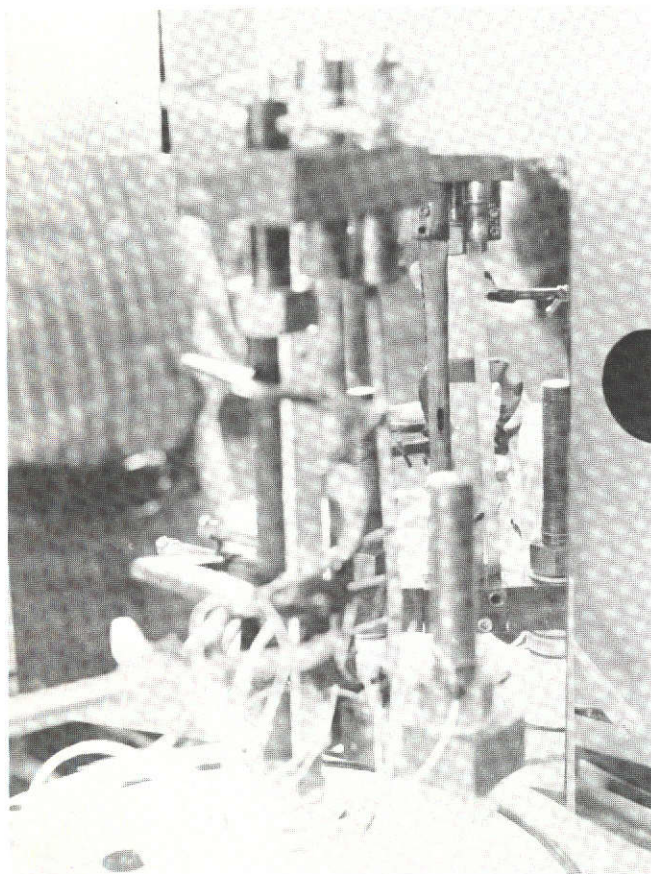
GP73-0587-22

Fig. 23 Mirror view of heated TD-NiCr strip sample

differed by more than 200°F (111 K); the probe opened at the thermocouple bead before higher temperatures could be reached. At the 1800°F (1256 K) level the MDRL 0.063 SP probe (Fig. 20) was approximately 250°F (139 K) low.

Figure 22 shows the #2 tack-welded thermocouple output exceeded the sleeved couple by 160°F (89 K) at the 1825°F (1269 K) level. Moving the ceramic sleeve 0.125 in. (0.318 cm) from the sample reduced the difference to only 25°F (14 K).

It was concluded from these tests that tack-welded thermocouples should be used to measure the sample temperatures for all the metallic specimen tests. Attempts were made initially to use 36 gauge thermocouple wire. However, the thermocouple-sample junctions were too weak

using this small [0.005 in. (0.0127 cm) diam] wire. The use of 28 gauge Pt-Pt 10% Rh standard grade thermocouple wire was then adopted since the series of experiments showed no appreciable difference in temperature measurement between 28 and 36 gauge tack-welded thermocouples (Fig. 21).

Various techniques were investigated for routing the tack-welded thermocouple wires from the test samples through the Silfrax back-up insulation. It was concluded that the best technique was to tack the individual wires in close proximity to each other, route them between the sample backface and Silfrax for approximately 0.25 in. (0.635 cm) in opposite directions, and then pass them through individual holes in the Silfrax that were drilled perpendicular to the sample.

The sample backface temperature histories at five locations are presented in Figs. A-12 through A-92 in Appendix B, Volume II of this report for each of the samples tested. Histories for cycles near 25, 50, 75, and 100 are presented for those samples cycled 100 times and near 15, 30, and 50 for those cycled only 50 times. Within 30 sec the samples reached essentially an equilibrium temperature.

Also shown in Appendix B are the in-depth insulator temperature histories as measured by thermocouples 0.375 in. (0.952 cm), 0.750 in. (1.905 cm), and 1.125 in. (2.857 cm) away from the sample. The temperature histories of the sample and insulator during all cycles were recorded on magnetic tape.

Typical temperature histories as measured by the in-depth thermocouples and by both spring-loaded and tack-welded thermocouples on the sample backface are shown in Figs. 24 and 25 for the DS-3 sample. The slow response of the spring-loaded thermocouples can be seen by comparing these two figures. This led to the thermocouple investigation described above and to the subsequent change to rapid response tack-welded thermocouples on the sample backface.
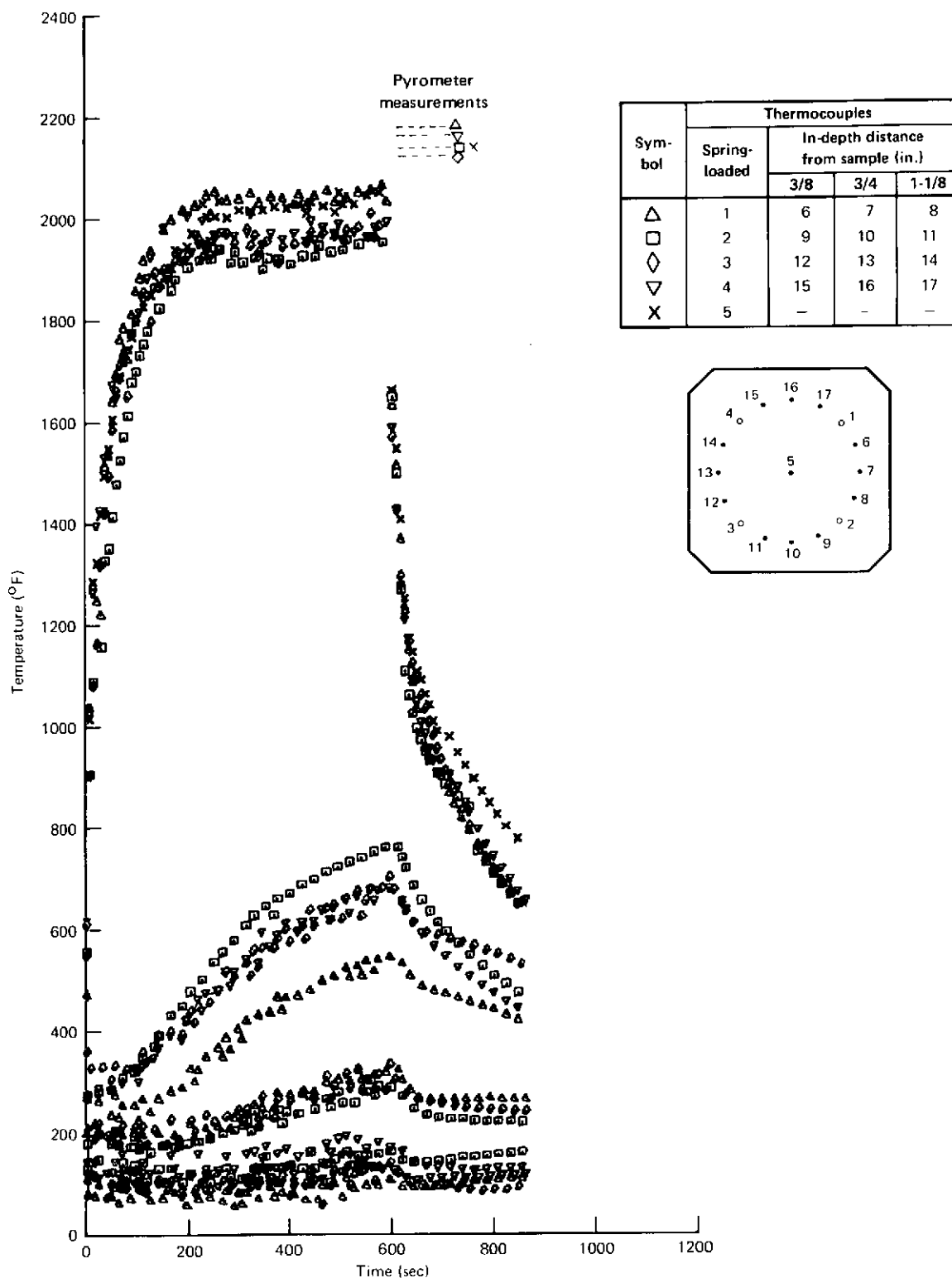
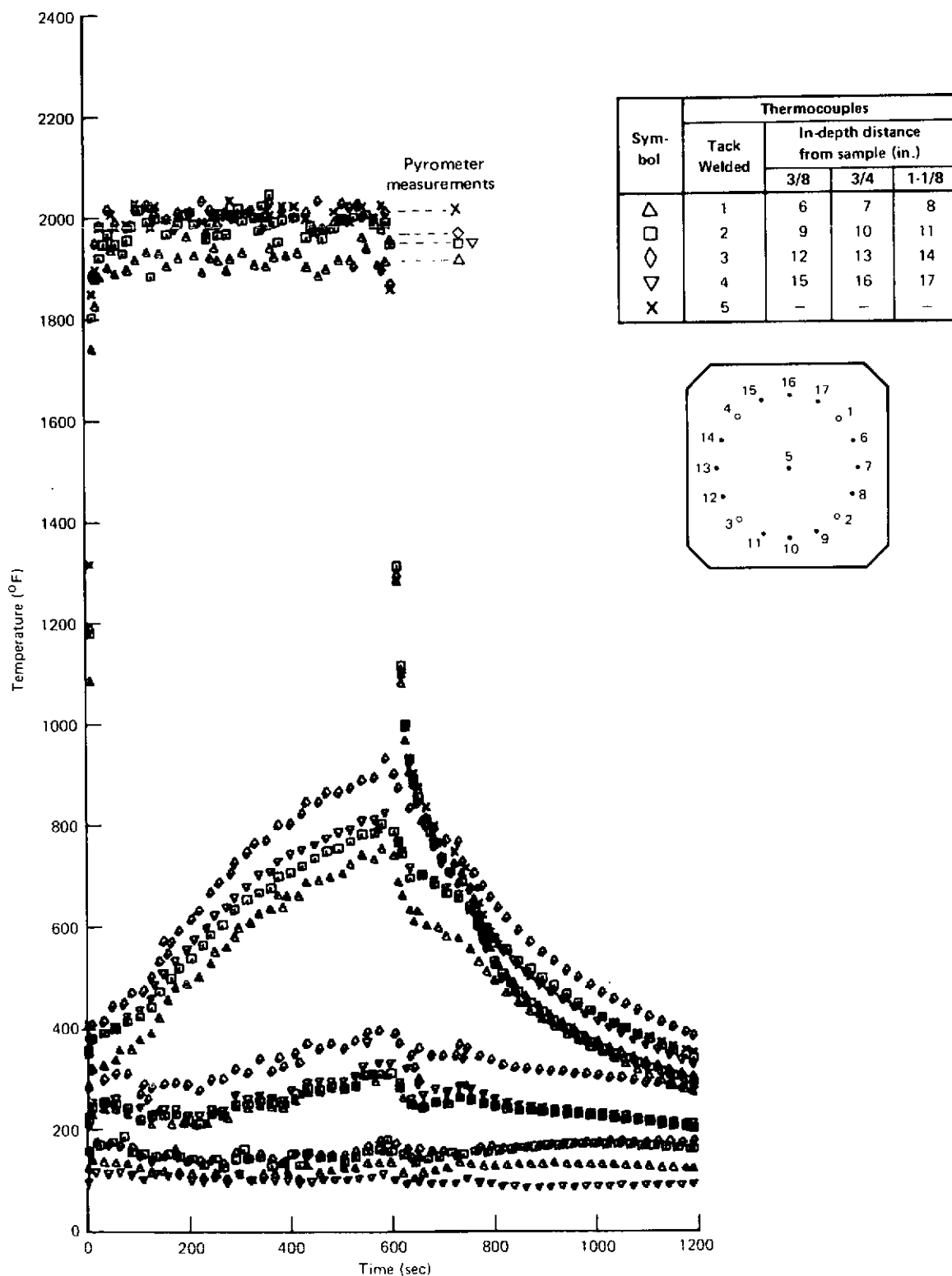Fig. 24 Typical temperature histories for DS-3 sample (cycle 27)

GP73-0587-24

MCDONNELL DOUGLAS

Symbol	Tack Welded	Thermocouples In-depth distance from sample (in.) 3/8	3/4	1-1/8
△	1	6	7	8
□	2	9	10	11
◊	3	12	13	14
▽	4	15	16	17
X	5	—	—	—

Fig. 25   Typical temperature histories for DS-3 sample (cycle 50)

GP73-0587-25

MCDONNELL DOUGLAS

6.2 Optical temperature measurements

6.2.1 Pyrometer

Figures 24 and 25 in this volume and Figs. A-12 through A-92 in Volume II show the pyrometer-measured temperature levels at five surface positions on the sample. These levels are indicated by the dashed lines with the symbols corresponding to the location of the backface thermocouples. The levels shown are an average of the two scans at each location and have been corrected for sample emittance and window transmittance. Good agreement was achieved between the pyrometer and backface thermocouple measurements for most samples. Periodic discrepancies were attributed to local surface emittance changes that were visually detected during tests. However, in Fig. 24 all the pyrometer measurements are considerably higher than the thermocouple data which were obtained using spring-loaded thermocouples. This gives further substantiation to the fact that the spring-loaded thermocouple measurements were in error.

Experiments were conducted to determine the effect of emittance control setting and window transmittance on the pyrometer-observed temperature measurements. Tests were made both during actual program cycles of the metallic samples and in a bench set-up using strip metallic samples.

During cycle 16 on metallic sample TD-9, the emittance control setting was varied from 0.1 to 0.9 and the pyrometer output was recorded. The indicated surface temperature decreased with an increase in emittance setting as expected. The indicated temperature (nominally 2000°F or 1367 K) decreased 120°F (67 K) as the emittance setting was increased from 0.5 to 0.9. All of the metallic samples tested had emittances in this range.

The difference between the pyrometer and thermocouple measured temperature is shown in Fig. 26 as a function of the emittance control
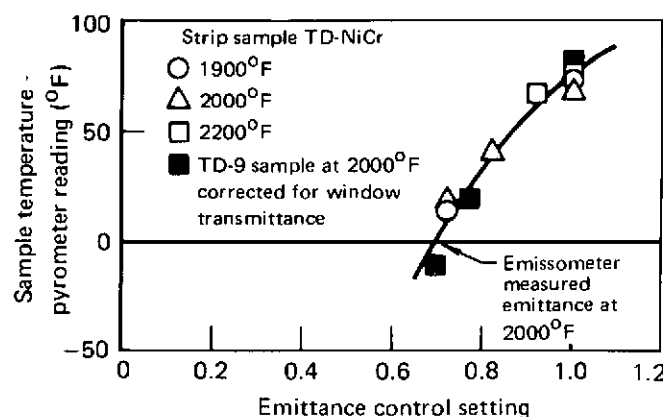

Fig. 26   Emittance control effects

GP73-0587-26

setting corrected for window transmission. Also shown in Fig. 26 are data taken from a strip sample in a bench test at temperatures from 1900 to 2200°F (1311 to 1478 K). These data show the sensitivity of the instrument to the emittance control setting and indicate good agreement between the emissometer measured emittance of 0.71 for TD-NiCr at 2000°F (1367 K) and the emittance control setting required for zero deviation between the pyrometer and corresponding backface thermocouple measurements.

Tests were made over a range of temperatures from 1900 to 2400°F (1311 to 1589 K) using a DS-NiCr strip sample 0.25 in. (0.635 cm) wide, 0.010 in. (0.0254 cm) thick, and 6.5 in. (16.5 cm) long in a bench experiment. The pyrometer was aligned through the same window used in the program tests. The pyrometer lens was 31 in. (78.7 cm) from the window and 43 in. (109 cm) from the strip sample. Tests were also made without the window to determine an effective transmittance.

The strip sample temperature was measured using a Pt-Pt 10% Rh thermocouple tack-welded to the backside. The sample temperature was increased in increments of 100°F (55.6 K) starting at 1900°F (1311 K). The emittance control setting was varied in increments of 0.05 over a range that encompassed agreement between the thermo-

couple and pyrometer measurements. Thus, the effective emittance was determined at each temperature level. This same technique was also used without the quartz window, and the combined data yielded the effective window transmittance. Figure 27 illustrates the effective window transmittance derived from these measurements. The scatter in the data is attributed to the low sensitivity of indicated temperature with the emittance control setting. For example, with a sample temperature of 2000°F (1367 K) the indicated temperature varied only 53°F (29.4 K) as the emittance control setting was varied from 0.47 to 0.66. Removing the window did not change the sensitivity appreciably.

The normal transmittance of the window was determined over a range of wavelengths using a spectrophotometer. These data are shown in Fig. 28. At the pyrometer characteristic wavelength (λ = 0.8 μm) the window transmittance was 0.87. This value is shown in Fig. 27 for comparative purposes.

The effect of pyrometer viewing angle was also investigated in this program. Tests were made over a range of temperatures from 1845 to 2228°F (1281 to 1493 K) using a TD-NiCr strip sample 0.50 in. (1.27 cm) wide, 0.010 in. (0.0254 cm) thick, and 6.5 in. (16.5 cm) long in a bench experiment. No window was used. The pyrometer viewing angle was varied from 15 to 90 deg (0.26 to 1.57 rad).
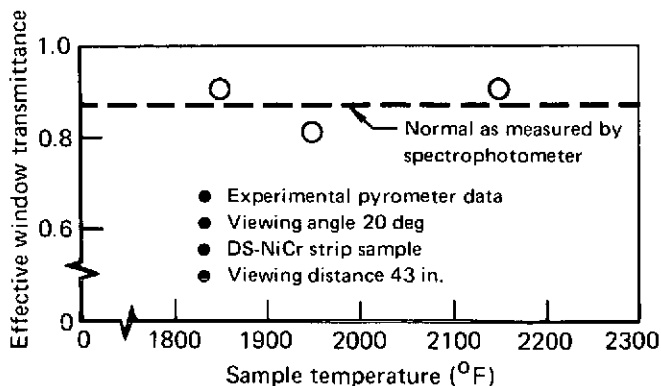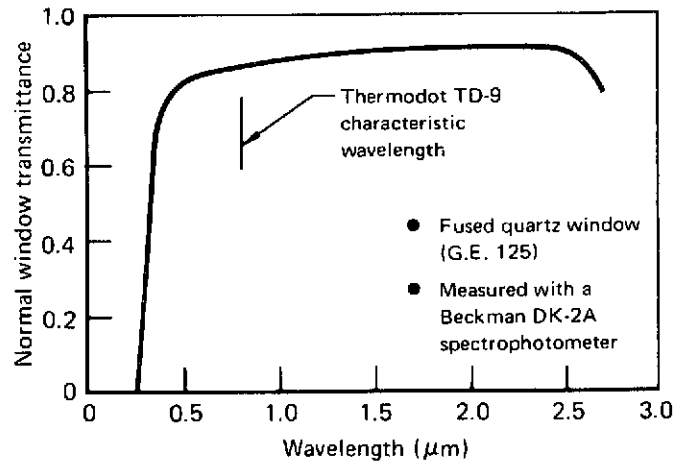

Fig. 28 Pyrometer window transmittance

GP73-0587-27

For an emittance setting of 0.72 (emissometer measured emittance), Fig. 29 shows that the viewing angle selection of 21 deg (0.37 rad) used for this program provided good agreement between the pyrometer reading and the sample thermocouple output for the full range of temperatures. Increasing the viewing angle resulted in a larger temperature deviation. The maximum deviation measured was 112°F (62 K) at a sample temperature of 1900°F (1311 K) and a viewing angle of 60 deg.

Lambert's cosine law states that the intensity of a plane source of radiation varies as the cosine of the angle of emission. Since the apparent visible brightness of a radiating surface depends on the radiant energy flux from that surface, the cosine law states that a blackbody has the same apparent brightness regardless of the angle from which it is viewed.

Real surfaces vary from this law depending upon the material. For most metals, as the angle between the direction of emission from a surface element and the normal to the surface (opposite of viewing angle) is increased, the emittance first increases and then decreases rapidly to zero at angles near parallel to the sample[5]. This trend is evident in Fig. 29.
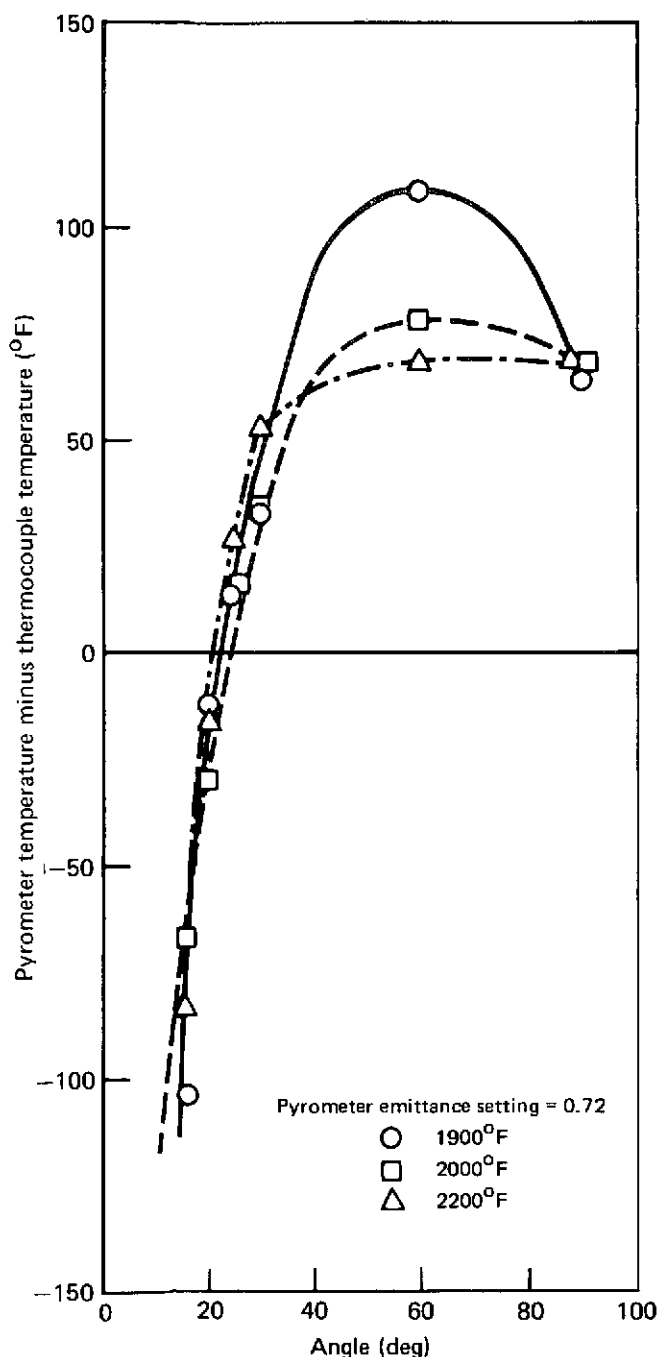

Fig. 27 Pyrometer window transmittance

Fig. 29 Temperature deviation as a function of viewing angle

GP73-0587-28

6.2.2 Model emittance

Total normal emittance measurements of all alloys tested for this program were made using the MDC

high temperature emissometer and the strip sample attachment described in Section 3.5.5.

Unoxidized samples 0.25 x 8.0 x 0.010 in. (0.64 x 20.3 x 0.0254 cm) of each material were repeatedly cycled from room temperature to typical test temperatures with the static air at a pressure of 10 Torr (1.3 x 10^3 N/m^2). Each heat cycle continued for approximately 10 min. A chromel-alumel thermocouple, spot-welded 0.5 in. (1.26 cm) below the sample center was used for sensing the strip temperatures. The sample emittance increased as the surface oxidized, and several heating and cooling cycles were conducted before a stable oxide layer developed.

Figure 30 illustrates the variation of total normal emittance of a TD-NiCr and DS-NiCr strip sample with time when at a temperature of 2000°F (1367 K). This behavior was characteristic of all the alloys tested. Each point shown is an average of three measurements.

Table 4 lists the final emittance values for the metallic samples at the various test temperatures. The product of the steady-state total normal emittance and the transmittance of the pyrometer observation port (G.E. 125 fuzed quartz) was used to establish the pyrometer emittance control setting.
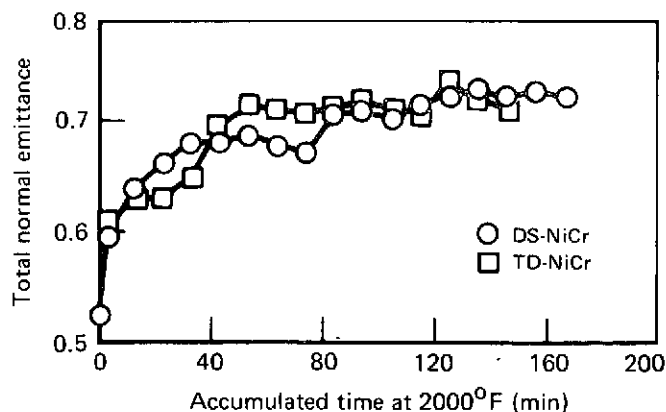

Fig. 30 Emittance history of TD-NiCr and DS-NiCr

GP73-0587-29

Table 4   Total normal emittance measurements

Material	Final emittance	No. of cycles	Sample temperature
TD-NiCr*	0.71	14	2000°F
TD-NiCr	0.70	11	2200°F
DS-NiCr	0.72	16	2000°F
TD-NiCrAl	0.49	15	2200°F
TD-NiCrAlY	0.50	15	2200°F
HS-188	0.75	20	1800°F
HS-188	0.77	9	2000°F
Hastelloy X	0.74	15	1800°F

*Emittance measurement not made at 1800°F but assumed to
be the same as at 2000°F.

GP73-0587-46

6.2.3 IR thermograms

At approximately the mid-point of each sample
test cycle, a thermogram was obtained showing
at least five isotherms on the sample surface.
During the test cycles on all samples up to cycle
33 on HS-1 and HS-2, the thermograms were
recorded using black and white Polaroid photo-
graphs. To provide more meaningful data, espe-
cially at the lower test temperatures, the thermo-
grams on subsequent tests were recorded using a
35 mm camera and color filter wheel which pro-
vided each isotherm with a characteristic color.
Typical thermograms resulting from each technique
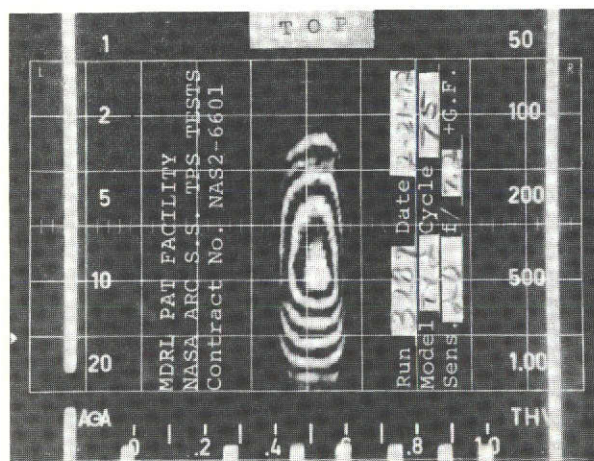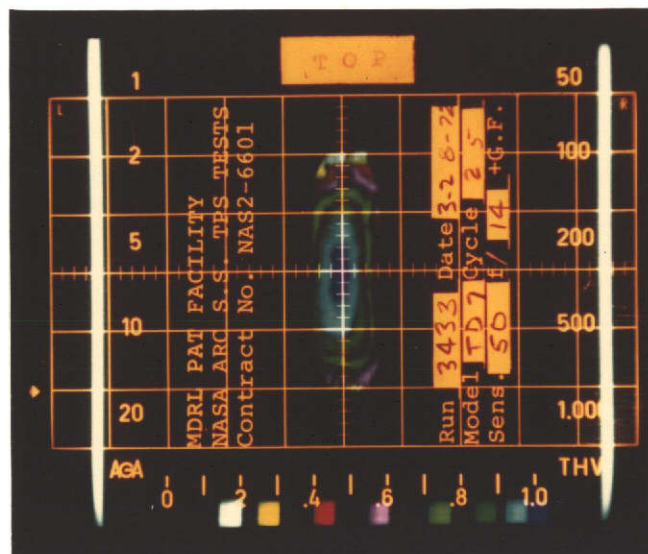are shown in Figs. 31 and 32.

Fig. 32   Typical color thermogram

A post-test calibration was performed to es-
tablish curves from which the surface temperature
could be obtained without determining the
absolute effects of background radiation from
the bow shock and arc radiance. The results of
this calibration are shown in Fig. 33 for the two
lens settings used during this test program. The
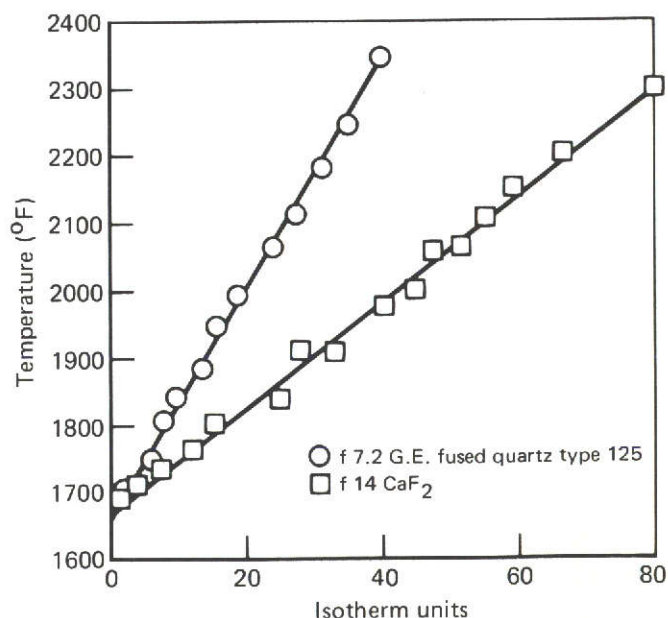figure can be utilized in the following manner:

Fig. 33   AGA thermovision system in situ calibration

Fig. 31   Typical black and white thermogram

GP73-0587-31

MCDONNELL DOUGLAS

1. Choose an isotherm (preferably the one at the model center) on a 35 mm color thermogram or black and white Polaroid that coincides with the location of a tack-welded thermocouple.

2. Determine the isotherm temperature as measured by the corresponding tack-welded thermocouple.

3. Determine the isotherm unit value on Fig. 33 corresponding to this temperature using the appropriate curve.

4. Choose any other isotherm location and its corresponding setting at the bottom scale of the thermogram. The difference between this setting and the setting for the previous isotherm multiplied by the sensitivity (shown on the thermogram) equals the Δi_0 to be subtracted from or added to the previously determined isotherm unit value.

5. With the new value of isotherm units, proceed vertically to the appropriate curve, and read the new temperature on the ordinate of Fig. 33.

Several checks were made by comparing temperatures determined from these curves with temperatures measured by the tack-welded thermocouples on various test models. The agreement was within ±1% when choosing isotherms within a 1.5 in. (3.81 cm) radius from the model center.

6.3 Thermal analysis

A thermal analysis was made of a metallic sample mounted in the water-cooled holder to predict:

- surface temperature distribution and history,
- in-depth back-up insulation temperature distribution and history,
- effects of cycling on the temperature distribution, and
- model holder sink effects.

Figure 34 illustrates the thermal model used in the calculations. The thermal properties used were those of a TD-NiCr metal sample backed by a 1.5 in. (3.8 cm) thick Silfrax insulator. The model was separated from the holder on the sides by 0.062 in. (0.157 cm) of Fiberfrax insulation. The water-cooled housing was assumed to have a 100°F (311 K) average wall temperature. Since the model has four identical quadrants, only one was analyzed.

The general heat transfer program "HEATRAN"[4] was used for these calculations. The thermal analyzer subprogram used was provided with subroutines for heat transfer calculations by the following modes:
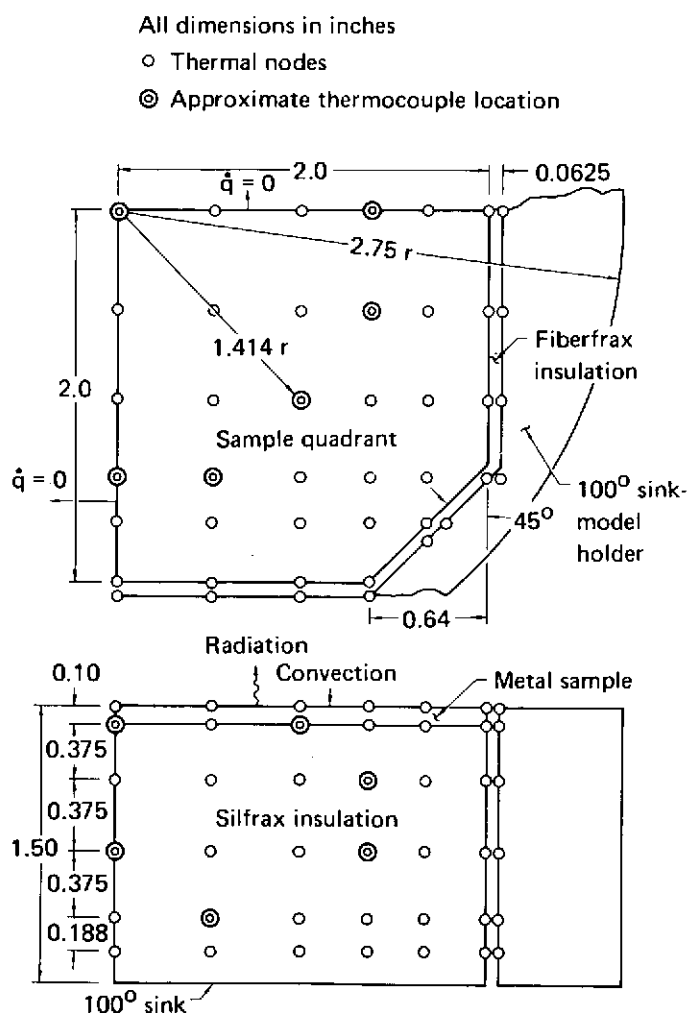
All dimensions in inches
o   Thermal nodes
◎   Approximate thermocouple location

Fig. 34   Thermal model of sample

1) heat storage,
2) conduction,
3) radiation,
4) heat addition or generation,
5) heat flux solution (inverse problem), and
6) convection and aerodynamic heating.

Modes 1, 2, 3, and 6 were used in this analysis. Two-dimensional transient heat transfer was considered and the nodes were modeled in rectangular coordinates. The program output was the temperature history at each specified node. A total of 258 nodes were used to completely define the model and insulator temperature history. Nodal planes were placed at the sample surface, sample back-face, on the model holder, and in the insulation as shown in Fig. 34.

Figure 35 compares measured temperature histories of sample TD-7 during cycle 50 with those predicted by the thermal analysis. The mid-side and mid-corner predictions are both on the same radius, but the mid-side point is closer to the cold holder wall and thus is at a lower temperature. The predicted in-depth temperatures are generally higher than the measured values. This could have been caused partially by a temperature difference between the sample and the front surface of the Silfrax insulator. Buckling of the sample would create an insulating air gap between the two. Radiation calculations assuming infinite parallel planes indicate a $50^\circ F$ (28 K) temperature difference would be sufficient to transfer 4% of the sample heat flux.

Another plausible explanation of the deviation could be the assumed Silfrax thermal conductivity. A value of 8.34×10^{-2} Btu/hr/ft/$^\circ$R (0.144 W/m K) was used for these calculations.

Using the measured insulation in-depth temperatures and the above thermal conductivity value, it was determined that a maximum of 4% of the incident heat flux was conducted through the insulation. A steady-state condition in the insulation was not reached in a 10 min heat pulse as

shown in Fig. 36. Higher in-depth insulator temperatures were achieved on each consecutive cycle after a cold start, but they never achieved steady-state during any heat pulse.

With a negligible heat loss through the back-up insulator, a good correlation was found to exist between the measured sample emittance and the incident heat flux required to obtain the same test temperature for different metallic materials. For instance, comparing the TD-NiCrAlY and TD-NiCr samples tested at $2200^\circ F$ (1478 K), the ratio of measured emittance was $0.50/0.70 = 0.72$ while the ratio of measured average heat flux values was $21.4/28.4 = 0.75$.

The sample surface temperature distributions varied from one sample to another. The sample shape had a strong effect. As the model surface flexed, the sample temperature fluctuated accordingly. In general, the sample temperatures were uniform within $\pm 5\%$.

The sample minimum cool-down temperature varied somewhat with the test temperature. Table 5 lists the range of cool-down temperatures for the three test temperature levels.

Table 5   Sample cool-down temperatures

Maximum sample temperature	10 Min cool-down temperature
$1800^\circ F$	$280\text{-}420^\circ F$
$2000^\circ F$	$270\text{-}450^\circ F$
$2200^\circ F$	$380\text{-}550^\circ F$

GP73-0587-166

6.4 Physical measurements

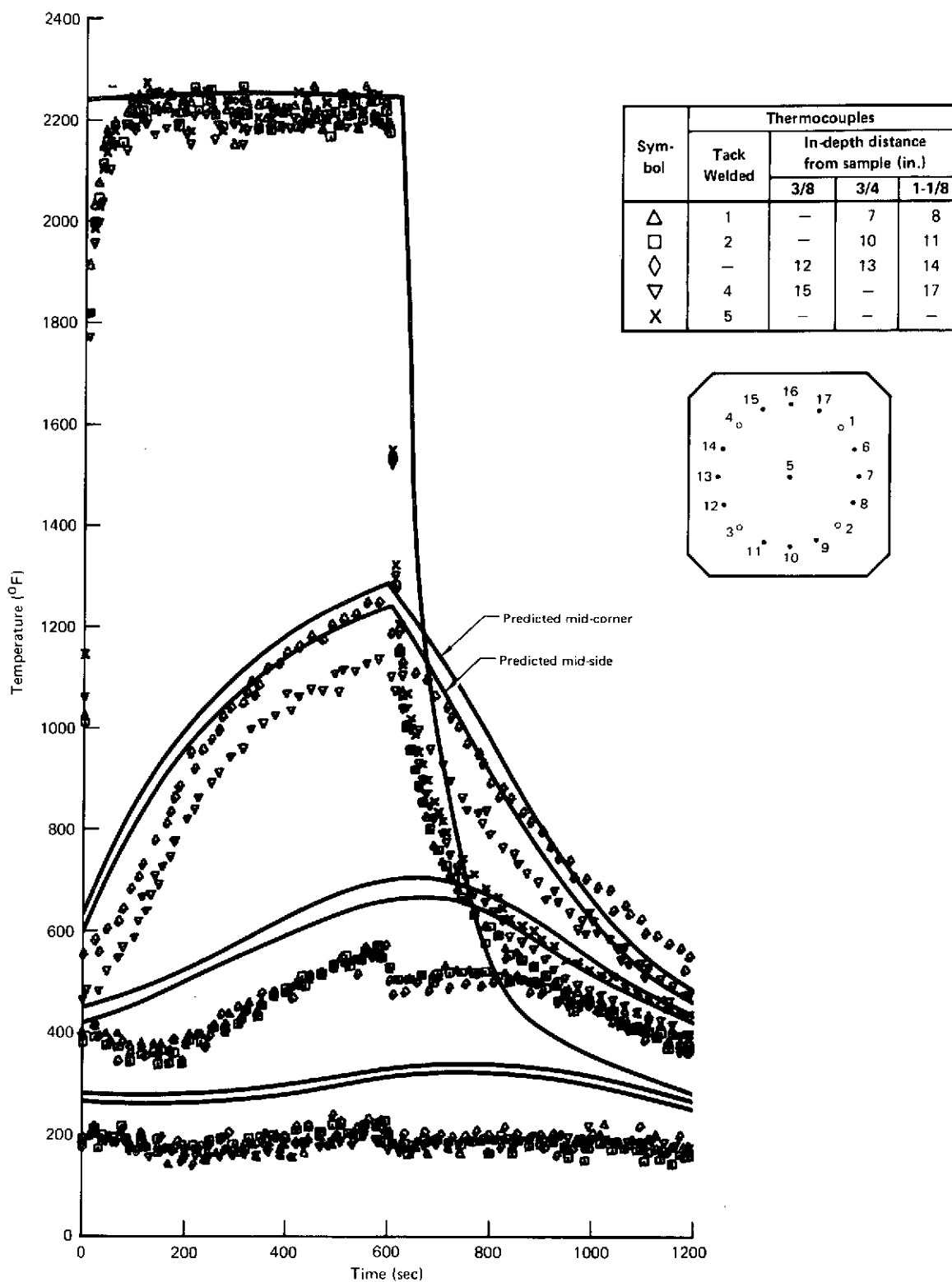Weight and thickness changes as a function of cycle number are shown for some samples in

Fig. 35 Typical temperature histories for TD-7 sample (cycle 50)
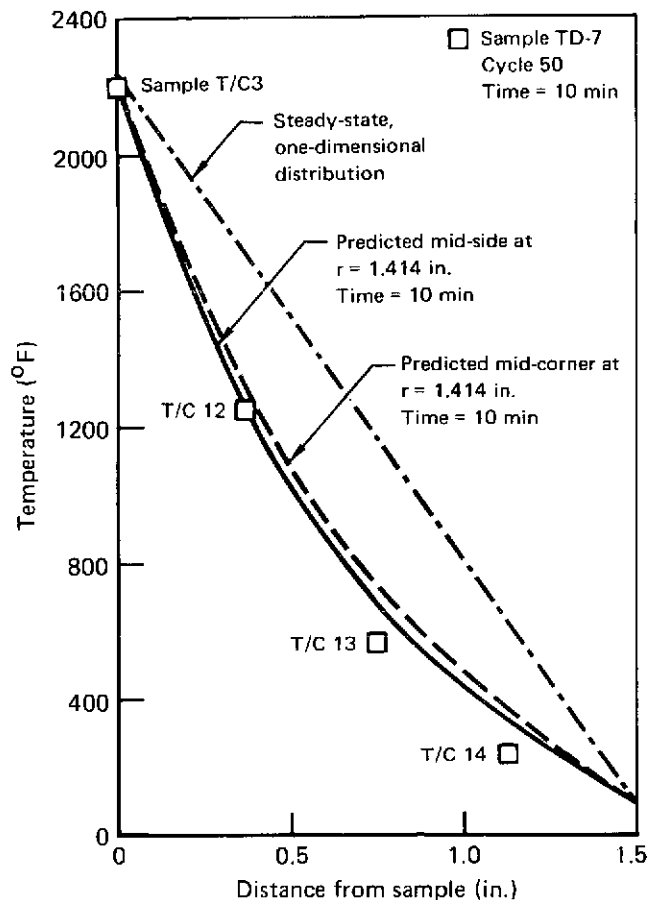
GP73-0587-33

Fig. 36 Back-up insulator temperature distribution

GP73-0587-34

Figs. 37 through 44. These physical measurements are also shown for each sample tested in Figs. A-93 through A-113 in Appendix C of Volume II of this report.

The marked change in the rate of weight loss and thickness increase shown in Figs. 37 and 38 for samples DS-3 and DS-4 occurred when the transition from spring-loaded to tack-welded thermocouples was made. As discussed in Section 6.1, it is probable that the sample temperature was considerably higher [> $100^\circ F$ (56 K)] than that indicated by the spring-loaded thermocouples when they were in use. Thus, a higher rate of weight and thickness change would be expected.

Although a thickness increase occurred during testing of the Hastelloy X samples (Figs. 39 and 40) this material displayed the greatest weight loss while being subjected to the lowest temperature environment. The TD-NiCrAl (Figs. 41 and 42) and TD-NiCrAlY (Figs. 43 and 44) materials showed the least change in weight, thickness, and physical appearance even though they were subjected to the highest temperature environment.
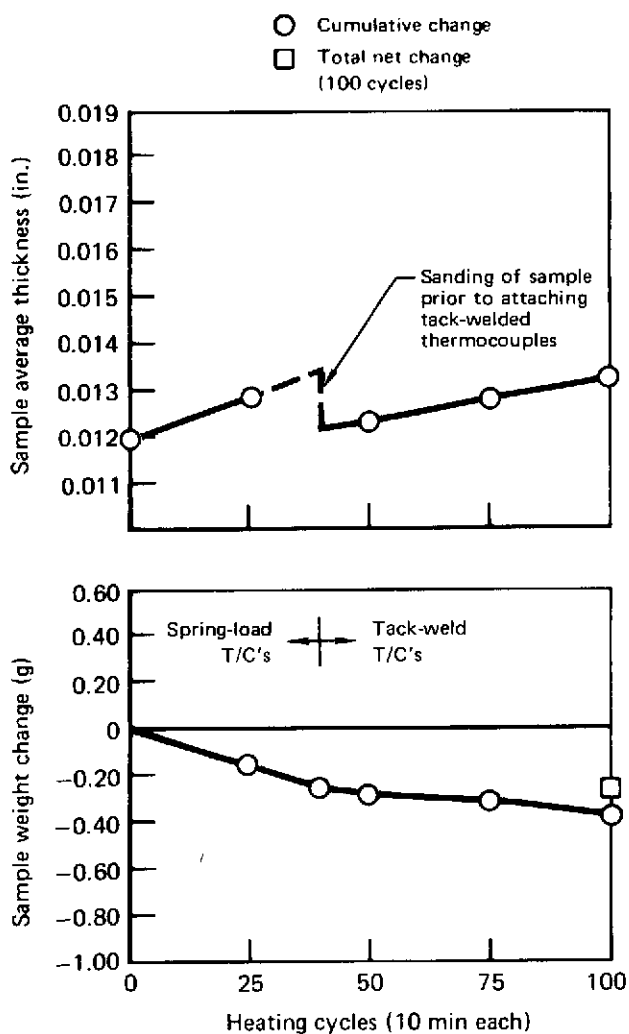
MCDONNELL DOUGLAS

Fig. 37 Sample weight and average thickness change

GP73-0587-35

Fig. 38 Sample weight and average thickness change

GP73-0587-36

Sample X-1
Temperature 1800°F

O Cumulative change
□ Total net change
   (100 cycles)

Sample X-2
Temperature 1800°F
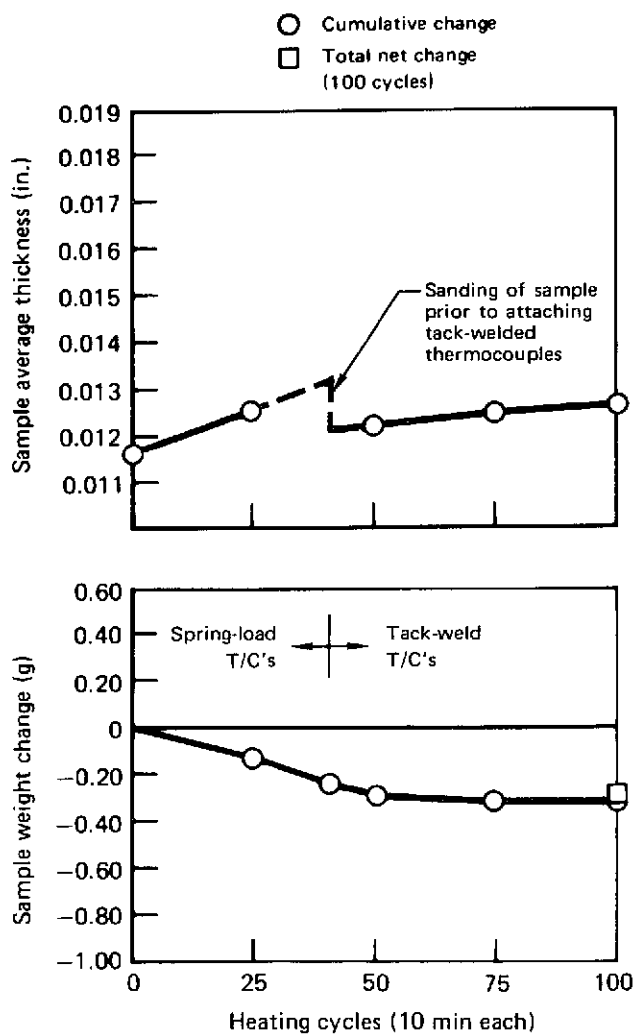
O Cumulative change
□ Total net change
   (100 cycles)

Fig. 39 Sample weight and average thickness change

GP73-0587-37

Fig. 40 Sample weight and average thickness change

GP73-0587-38

MCDONNELL DOUGLAS

Sample TAL-1
Temperature 2200°F

○ Cumulative change
□ Total net change
(100 cycles)

Sample TAL-2
Temperature 2200°F

○ Cumulative change
□ Total net change
(100 cycles)
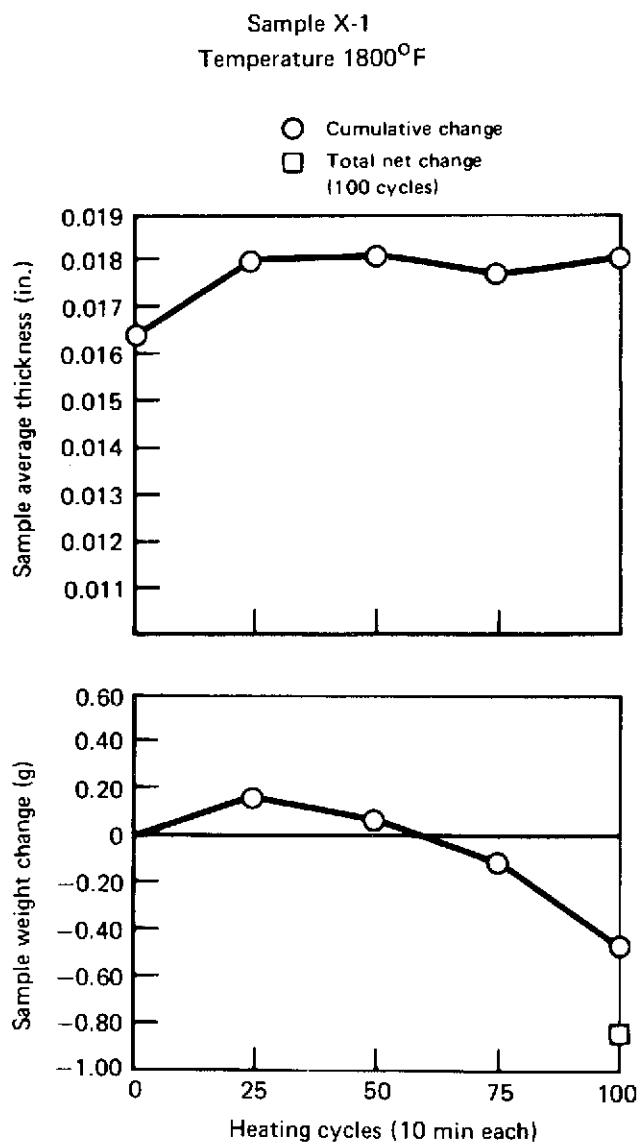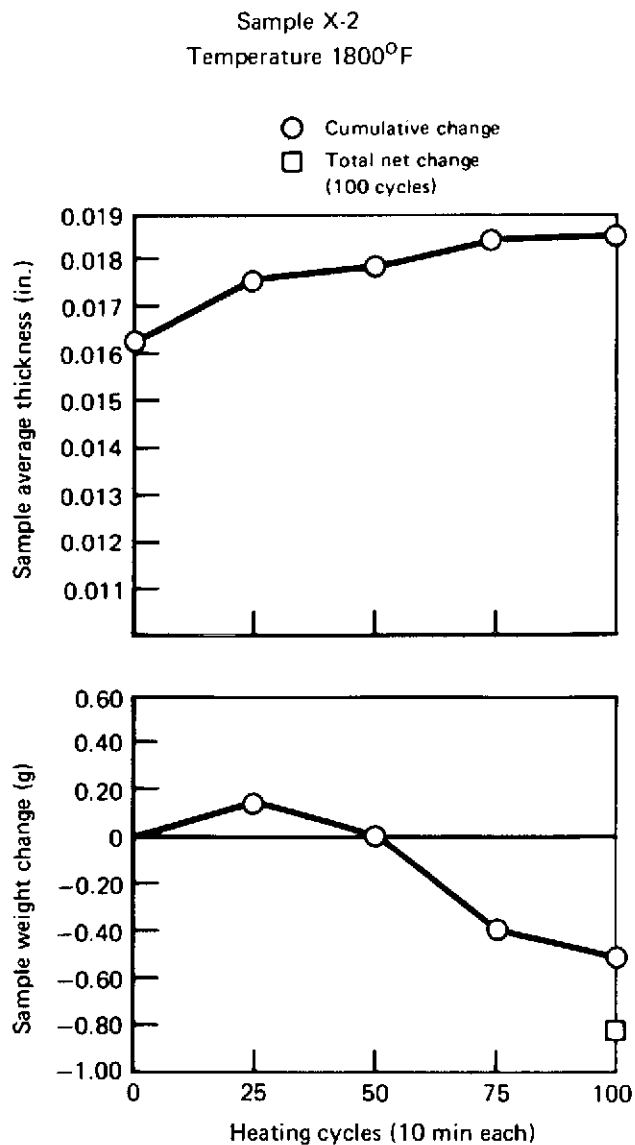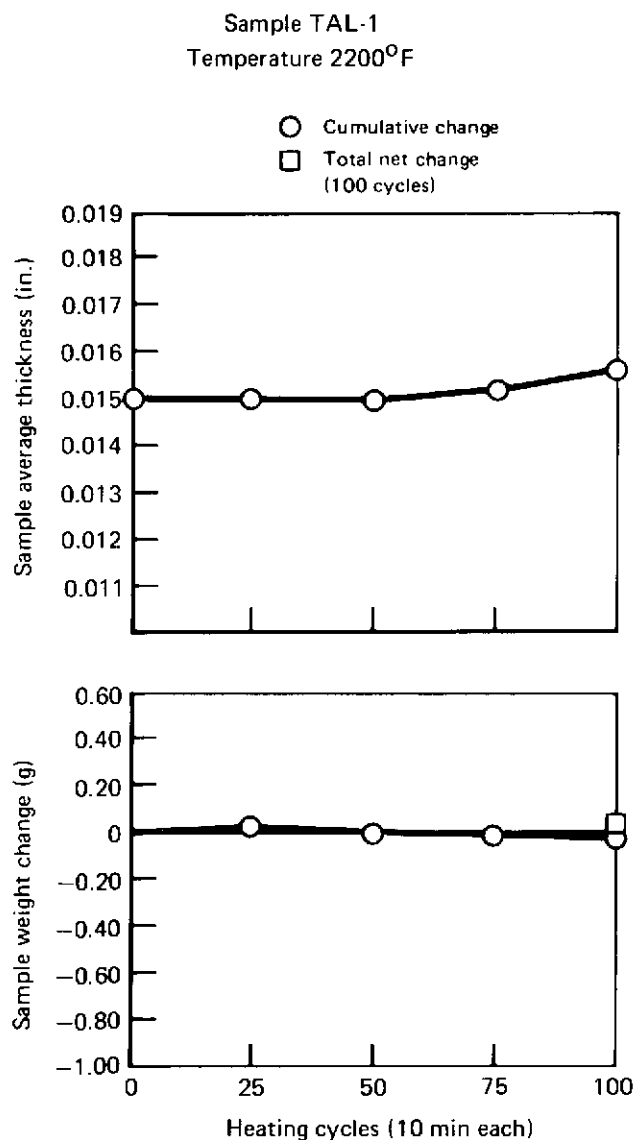
Fig. 41 Sample weight and average thickness change

GP73-0587-39

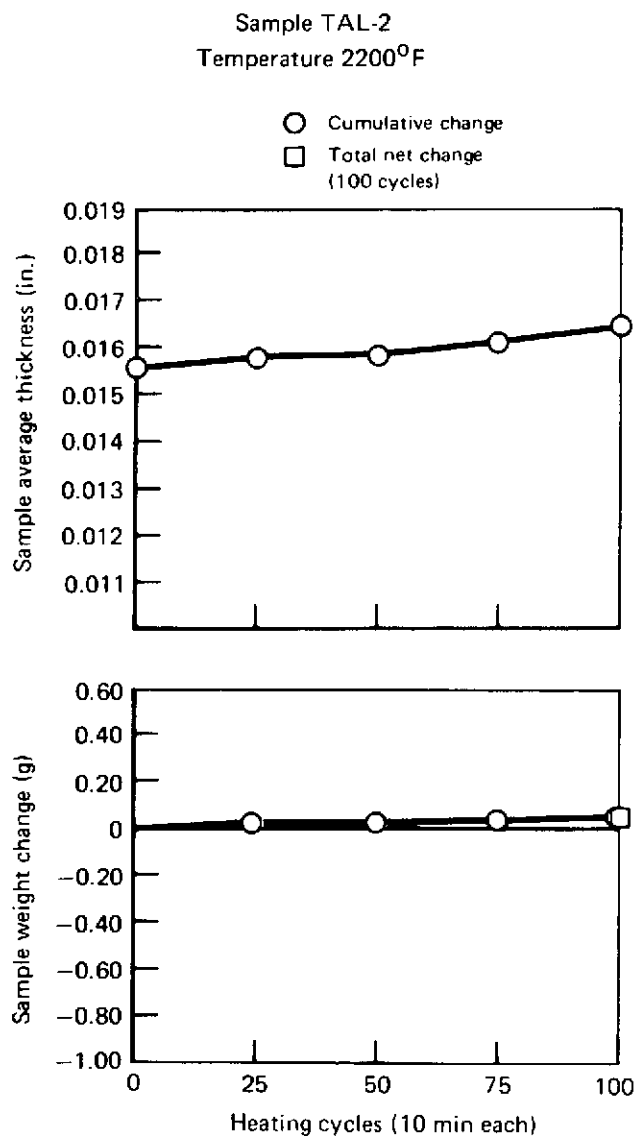Fig. 42 Sample weight and average thickness change

GP73-0587-40

MCDONNELL DOUGLAS
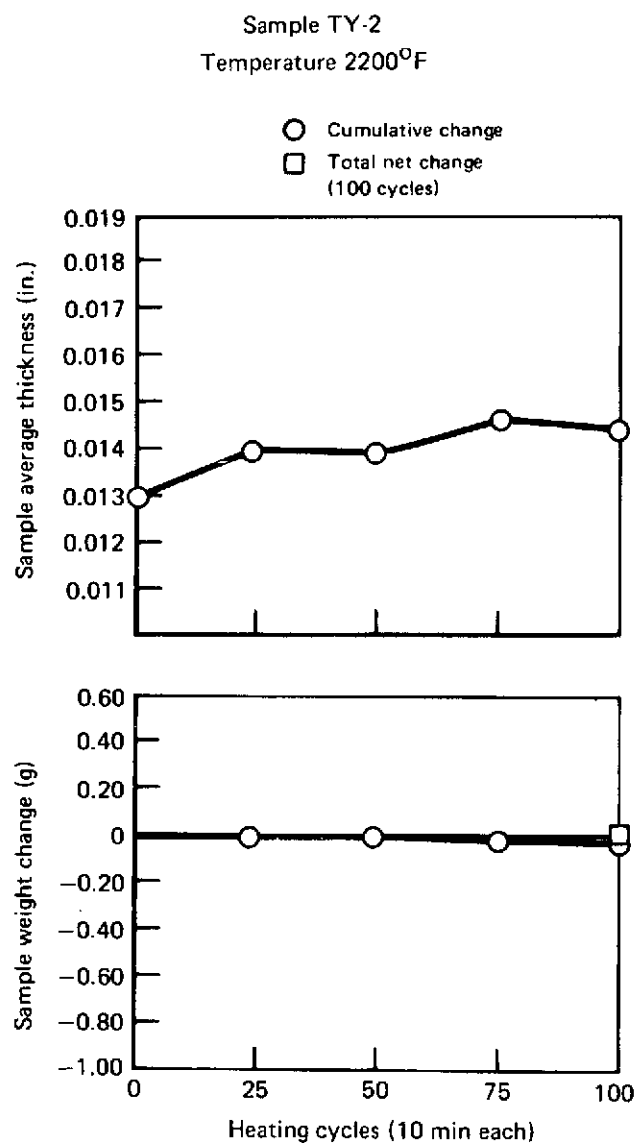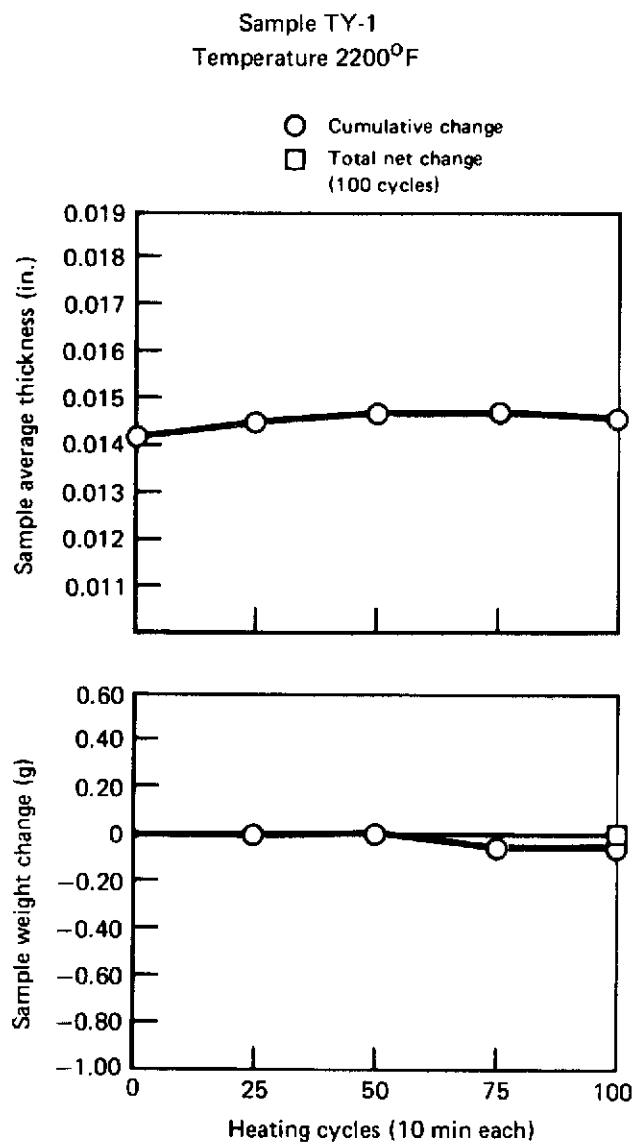
Fig. 44 Sample weight and average thickness change

Fig. 43 Sample weight and average thickness change

MCDONNELL DOUGLAS

7 Concluding remarks

Metallic materials were evaluated for the space shuttle thermal protection system (TPS) by cyclical testing of samples (up to 100 times each for 10 min each test cycle) in a hypervelocity oxidizing atmosphere. A total of 325 sample test hours were conducted in an arc heater facility on 21 metallic samples fabricated from five nickel base alloys and one cobalt base alloy. The tests were conducted at temperatures from 1800 to 2200°F (1256 to 1478 K) at a nominal impact pressure of 6 Torr (800 N/m^2) and an arc heater average exit enthalpy of 4000 Btu/lb (9.3 x 10^6 J/kg) with no sample failures.

Some conclusions drawn from this test program include:

1. It was possible to obtain 70% of the physical nozzle exit area as a test stream with a measured heat flux uniformity within ±10% and pressure within ±5% at Mach 4.6.

2. Direct contact surface temperature measurements indicated significant response and magnitude differences between tack-welded and spring-loaded thermocouples with the tack-welded thermocouples being more accurate. Errors of several hundred degrees were found in various spring-loaded thermocouple designs. The response of the tack-welded thermocouples was much faster than the spring-loaded thermocouples and agreed well with the pyrometer response.

3. Optical temperature measurements made using a pyrometer showed nominal agreement within 5% of the tack-welded thermocouple measurements. A scanning infrared imaging system was used to measure the sample front face temperature distribution. This was the first time this system had been used in this application. The distribution of surface temperature as determined by this system was essentially uniform (±5%) and in equilibrium over nearly the entire 10 min heat pulse.

4. Insulation heat transfer never reached the steady state, one-dimensional mode during the 10 min heat cycles. Measurements from the imbedded thermocouples in the Silfrax back-up insulator indicated that the maximum heat loss through the insulator was 4% of the incident heat flux. The temperature of the sample after a 10 min cool down was approximately 400°F (477 K).

5. A good correlation was found to exist between the measured sample emittance and the incident heat flux required to obtain the same test temperature for different metallic materials. Comparing the TD-NiCrAlY and TD-NiCr samples tested at 2200°F (1478 K), the ratio of measured emittances was 0.50/0.70 = 0.72 while the ratio of measured average heat flux values was 21.4/28.4 = 0.75.

6. Although a thickness increase occurred during testing of the Hastelloy X samples, this material displayed the greatest weight loss while being subjected to the lowest temper-

ature environment. The TD-NiCrAl and TD-NiCrAlY materials showed the least change in weight, thickness, and physical appearance even though they were subjected to the highest temperature environment.

8 Symbols

c	-	Constant	R_{max}	-	Maximum model radius
d_{ex}	-	Nozzle exit diameter	s	-	Surface distance along nozzle wall
d_m	-	Model diameter	t	-	Thickness of sample
E	-	Arc voltage	V	-	Free stream gas velocity
h_{ex}	-	Gas enthalpy at nozzle exit	W	-	Metallic model edge width
I	-	Arc current	x	-	Axial distance from nozzle exit
Δi_o	-	Object isotherm difference	δ	-	Boundary layer thickness
$\dot{m}_1$	-	Primary air flow rate	λ	-	Wavelength
$\dot{m}_2$	-	Secondary air flow rate	ρ	-	Density
M	-	Mach number	μ	-	Viscosity
P_T'	-	Model surface pressure	Subscripts		
$\dot{q}$	-	Heat flux to surface	r	-	Evaluated at Eckert's reference temperature
R_1	-	Core radius at nozzle exit			
R_b	-	Model bend radius	av	-	Average value
R_{ex}	-	Nozzle exit radius	$\mathcal{C}_L$	-	Centerline value

9 References

1. D.W. Land, R.R. Williams, and W.A. Rinehart, "Testing Superalloys at 2000 (1367) and 2200°F (1478 K) in a Mach 4.6 Airstream," NASA CR 120913 (April 1972).

2. A.F. Burke and K.D. Bird, "The Use of Conical and Contoured Expansion Nozzles in Hypervelocity Facilities," Cornell Aeronautical Laboratory Report No. 112, revised (July 1962).

3. T.H. Allen, "A Device for Accurate Measurement of Total Normal Emittance Under Simulated Reentry Conditions," AIAA 6th Thermophysics Conference, Tullahoma, Tennessee (April 1971).

4. "KBDR General Heat Transfer Program User's Manual," McDonnell Douglas Report A0613 (September 1970).

5. W.D. Wood, H.W. Deem, and C.F. Lucks, "Emissivity and Emittance, What Are They?" Battelle Memorial Institute DMIC No. 72 (November 1960).

10 Distribution list

NASA Headquarters
Washington, D.C. 20546
   F.J. DeMeritte, Code RV
   G.C. Deutsch, Code RW
   J.J. Gangler, Code RWM
   W.C. Hayes, Code RS
   J. Maltz, Code RWM
   N.G. Peil, Code MHE

NASA Ames Research Center
Moffett Field, California 94035
   D.R. Chapman, M/S 229-3
   G. Goodwin, M/S 200-4
   H. Goldstein, M/S 234-1
   H.K. Larson, M/S 234-1
   C.R. Nysmith, M/S 229-5
   D.P. Williams, M/S 240-1

NASA John F. Kennedy Space Center
Florida 32899
   S.S. Ewing, Code LS-ENG-22
   N.R. Koenig, Code TS-NTS-2
   M.G. Olsen, Code DD-MDD-1

NASA Langley Research Center
Hampton, Virginia 23365
   R.A. Anderson, M/S 188
   W.A. Brooks, M/S 188M
   R.R. Howell, M/S 208
   B.A. Stein, M/S 188A
   L.F. Vosteen, M/S 206

NASA Lewis Research Center
Cleveland, Ohio 44135
   R.W. Hall, Code 5550
   S.R. Levine, Code 0300
   J.P. Merutka, Code 5540
   H.B. Probst, Code 5560

NASA Manned Spacecraft Center
Houston, Texas 77058
   C.M. Grant, Code JM2
   D.H. Greenshields, Code ES
   R.E. Johnson, Code ES5
   J.A. Smith, Code ES3
   G. Strouhal, Code ES3

NASA George C. Marshall Space Flight Center
Alabama 35812
   C.E. Cataldo, Code S&E-ASTN-MX
   F. Huneidi, Code S&E-ASTN-PT
   W.A. Riehl, Code S&E-ASTN-M

Wright Patterson Air Force Base
Ohio 45433
   N. Geyer, FOS MTLS Lab
   W.H. Goesch, Flight Dyn Lab

Aerotherm Corp./Louis J. Alpinieri
AVCO Corp./Irwin J. Metcalfe
Battelle Columbus Labs./Phillip N. Livingstone
The Boeing Company/Eugene F. Styer
Chrysler Corp./Space Division/C. E. Tharratt
General Dynamics Corp./E. O. A. Naumann
General Electric Company/W. Daskin
Grumman Aerospace Corp./Fred Raymes
Lockheed Missiles and Space Co./John S. Milton
Martin Marietta Corp./Charles R. Gunnison
McDonnell Douglas Corp./Don Kummer
North American Rockwell Corp./Pat Hanifan

DOCUMENT CONTROL DATA - R & D

(Security classification of title, body of abstract and indexing annotation must be entered when the overall report is classified)

1. ORIGINATING ACTIVITY *(Corporate author)*	2a. REPORT SECURITY CLASSIFICATION
McDonnell Douglas Research Laboratories P.O. Box 516 St. Louis, Missouri 63166	Unclassified
	2b. GROUP

3. REPORT TITLE

CYCLICAL TESTS OF SELECTED SPACE SHUTTLE TPS METALLIC MATERIALS IN A PLASMA ARC TUNNEL

4. DESCRIPTIVE NOTES *(Type of report and inclusive dates)*

Final Report

5. AUTHOR(S) *(First name, middle initial, last name)*

Walter A. Rinehart, Donald W. Land, James H. Painter, Ronald A. Williamson

6. REPORT DATE	7a. TOTAL NO. OF PAGES	7b. NO. OF REFS
June 1972		5
8a. CONTRACT OR GRANT NO. NAS2-6601	9a. ORIGINATOR'S REPORT NUMBER(S)	
b. PROJECT NO.	MDC Q0473	
c.	9b. OTHER REPORT NO(S) *(Any other numbers that may be assigned this report)*	
d.	NASA CR 114459	

10. DISTRIBUTION STATEMENT

This document may be further distributed by any holder only with specific prior approval of NASA Ames.

11. SUPPLEMENTARY NOTES	12. SPONSORING MILITARY ACTIVITY
	NASA Ames Research Center Moffett Field, California 94035

13. ABSTRACT   The work described in this report concerned the cyclical thermal evaluation of selected space shuttle thermal protection system (TPS) metallic materials in a hypervelocity oxidizing atmosphere that approximated an actual entry environment. A total of 325 sample test hours were conducted in the McDonnell Douglas Research Laboratories (MDRL) Plasma Arc Tunnel (PAT) facility on 21 superalloy metallic samples at temperatures from 1800 to 2200°F (1256 to 1478 K) without any failures. The 4 x 4 in. (10.2 x 10.2 cm) samples were fabricated from five nickel base alloys and one cobalt base alloy. Eighteen of the samples were cycled 100 times each and the other three samples 50 times each in a test stream emanating from an 8 in. (20.3 cm) diam exit, Mach 4.6, conical nozzle. The test cycle consisted of a 10 min heat pulse to a controlled temperature followed by a 10 min cooldown period.

Measurements of sample temperature were obtained with both physical and optical techniques. Each sample was instrumented on the backface with five tack-welded thermocouples. Measurements of weight and thickness changes were made at periodic intervals for each sample. The TD-NiCrAl and TD-NiCrAlY materials showed the least change in weight, thickness, and physical appearance even though they were subjected to the highest temperature environment.

14. KEY WORDS	LINK A		LINK B		LINK C	
	ROLE	WT	ROLE	WT	ROLE	WT
arc tunnel						
metallic sample						
model holder						
insulator						
test cycle						
heat flux						
pressure						
surface temperature						
thermocouple						
emittance						

UNCLASSIFIED
Security Classification